Electronic Supplementary Material (ESI) for ChemComm.

Real-time visualizing the fluctuations of hypobromic acid with AIE fluorescent probes during myocardial ischemia-reperfusion injury

Jian Zhang,[#] Yingying Xie,[#] Jushuai Ma, Kaiqiang Liu, Yunshu Ding, Yong Li, Xiaoyun Jiao, Xilei Xie, Xu Wang,* and Bo Tang*

†College of Chemistry, Chemical Engineering and Materials Science, Collaborative Innovation Center of Functionalized Probes for Chemical Imaging in Universities of Shandong, Key Laboratory of Molecular and Nano Probes, Ministry of Education, Shandong Provincial Key Laboratory of Clean Production of Fine Chemicals, Shandong Normal University, Jinan 250014, P. R. China.

E-mail: tangb@sdnu.edu.cn, wangxu@sdnu.edu.cn

1. Materials and Instruments

All chemicals were purchased from Adamas Reagent, Ltd. (China), and analytical grade solvents were used without further purification. All aqueous solutions were prepared using ultrapure water (ultrapure water, 18 MΩ cm^{-1}). MTT was purchased from Sigma Corporation, column chromatography silica gel (200-300 mesh) was purchased from Qingdao Haiyang Reagent Co., Ltd. The DMEM medium, penicillin/streptomycin and fetal calf serum was purchased from Gibco Corporation. Estradiol benzoate (E2), D/L-propargyl glycine (PPG) and fulvestrant were purchased from Aladdin. The AnaerPouch is purchased from Boster. H9C2 cells were purchased from Procell Life Science & Technology Co., Ltd.

Fluorescence data was measured by a F-4700 fluorescence spectrophotometer (Hitachi) at room temperature (slit for QM-S: 5.0 nm, 10.0 nm; slit for QM-Se: 5.0 nm, 10.0 nm). The absorption spectra were measured on a UV-1700 spectrophotometer (Shimadzu, Japan). The mass spectra were obtained by Maxis MHR-TOF ultra-high resolution quadrupole time of flight mass spectrometer (Bruker Germany). The ^{1}H NMR and ^{13}C NMR spectra were acquired on a nuclear magnetic resonance spectrometer (400 MHz, Bruker Co., Ltd., Germany). The δ value represents the shift of the spectrum relative to TMS ($(CH_3)_4Si$ = 0.00 ppm). The LC-Mass were performed on a high-performance liquid chromatography-mass spectrometer (LC-16, Shimadzu, Japan). Transmission electron microscopy (TEM) images were taken on a JEM-1011 electron microscope (JEOL, Japan) at an accelerating voltage of 100 kV. Dynamic light scattering (DLS) measurements were performed on a Malvern zeta sizer Nano-ZS90. Confocal imaging data were obtained on TCS SP8 confocal laser scanning microscope (CLSM, Leica Co., Ltd., Germany). The data of MTT experiment was measured with a microplate reader (TRITURUS).

Preparation of various interference substances. All reagents were used right after they were ready. Cys, Hcy, GSH and vitamin C (Vc) were all used as received. S^{2-} and HSO_3^- were all used as their sodium salt and prepared as the stock solutions.

K^+, Na^+, Mg^{2+}, Ca^{2+}, Cu^{2+}, Co^{2+}, Fe^{2+}, Fe^{3+} and Al^{3+} were all used as their chloride salt and prepared as the stock solutions. All these compounds were commercial

available with analytical purity and used directly.

We prepared reactive oxygen species (ROS) as follows:

Hypobromous acid (HOBr): To ultrapure water (7.5 mL) was added liquid bromine (50.0 μL), the mixture was titrated with $AgNO_3$ solution at 0 ℃ until the solution was colorless. After filtering, the filtrate was reserved for use. UV-Vis spectra was performed to measure the absorbance at 260 nm and [HOBr] determined by Lambert-Beer's law (ε_{260} = 160 L M^{-1} cm^{-1}).

Peroxynitrite ($ONOO^-$): hydrochloric acid (0.6 M) was added to the mixture of $NaNO_2$ (0.6 M) and H_2O_2 (0.7 M), then NaOH (1.5 M) was added. The resulted faint yellow solution was split into small aliquots and stored at lower than -20 °C. The concentration of the prepared peroxynitrite was determined by testing the absorption of the solution at 302 nm. The extinction coefficient of $ONOO^-$ solution is 1670 M^{-1} cm^{-1} at 302 nm. $C_{ONOO^-} = Abs_{302nm}/1.67$ (mM).

Hydroxyl radical (•OH) was prepared by the reaction of Fe^{2+} with H_2O_2 (1:6), and the concentration of •OH is equal to the concentration of Fe^{2+}.

Singlet oxygen ($^1O_2$) was prepared in situ by addition of the H_2O_2 stock solution into a solution containing 10 eq of NaClO.

Superoxide solution ($O_2^{\bullet-}$) was prepared by adding KO_2 to dry dimethylsulfoxide and stirring vigorously for 10 min.

Hydrogen peroxide (H_2O_2) was diluted appropriately in water. The concentration of H_2O_2 was determined by measuring the absorbance at 240 nm with a molar extinction coefficient of 43.6 M^{-1} cm^{-1}.

Nitric oxide (NO) was used from a stock solution prepared by sodium nitroprusside.

Hypochlorous acid (HClO) was obtained by diluting commercial aqueous solutions. The concentration was determined by measuring the absorbance at 292 nm with a molar extinction coefficient of 391 M^{-1} cm^{-1}.

2. Fluorescence analysis

Fluorescence titration profiles of the probe were constructed by mixing QM-S (10.0 μM) with different level of HOBr (0-100.0 μM) in PBS buffer solution (1 % DMSO, 100 mM, pH=7.4, 37 °C). The measurement was carried out at $\lambda_{ex}/\lambda_{em}$ = 420/600 nm for QM-S. Fluorescence titration profiles of the probe were constructed by mixing QM-Se (10.0 μM) with different level of HOBr (0-50.0 μM) in PBS buffer solution (1 % DMSO, 100 mM, pH=7.4, 37 °C). The measurement was carried out at $\lambda_{ex}/\lambda_{em}$ = 420/620 nm for QM-Se. The specificity experiments of QM-S/QM-Se towards HOBr were carried out by incubation of the probe with HOBr and other biorelevant species, including reactive oxygen and nitrogen species (•OH, $^1O_2$, $O_2^{\cdot-}$, H_2O_2, HClO, NO, $ONOO^-$), reactive sulfur species (GSH, Cys, Hcy and S^{2-}), reductive species (HSO_3^-, and Vc), and metal ions (K^+, Na^+, Mg^{2+}, Ca^{2+}, Cu^{2+}, Co^{2+}, Fe^{2+}, Fe^{3+} and Al^{3+}) in PBS buffer solution (1 % DMSO, 100 mM, pH=7.4, 37 °C). The kinetic studies of fluorescence responses were performed by incubating the probe with HOBr at $\lambda_{ex}/\lambda_{em}$ = 420/600 nm for QM-S and $\lambda_{ex}/\lambda_{em}$ = 420/620 nm for QM-Se respectively.

Determination of Fluorescence Quantum Yield. The absorbance of QM-S/QM-Se and the corresponding product was adjusted to ca. 0.05. The emission spectra were obtained by exciting with corresponding maximal excitation wavelength and the integrated areas of the fluorescence spectra were calculated. The fluorescence quantum yield was determined by comparing the integrated emission intensity of the test samples with that of a solution of Rhodamine B (the fluorescence standard, Φ_F = 0.97 in EtOH) and calculated by following equation.

$$\Phi_{F(X)} = \Phi_{F(S)} \times \left(\frac{F_X}{A_X}\right) \times \left(\frac{A_S}{F_S}\right) \times \left(\frac{n_X}{n_S}\right)^2$$

where Φ_F is the fluorescence quantum yield, A is the absorbance at the excitation wavelength, F is the area under the emission curve, and n is the refractive index of the solvents used. Subscripts S and X refer to the standard and the samples to be tested, respectively.

3. Synthesis and characterization of QM-S/QM-Se

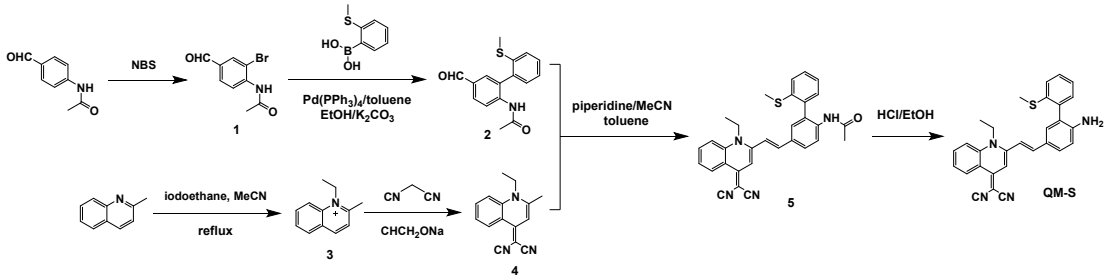

Fig. S1 Synthesis procedure of QM-S.

Synthesis of compound 1 [1]

NBS (1.43 g, 8.95 mmol) was dissolved in 40 mL water, and N-(4-formylphenyl) acetamide (1.003 g, 6.15 mmol) was added to NBS solution, and the mixture was stirred at room temperature for 48 h. The reaction mixture was filtered, the solid was collected, the excess solvent was removed under reduced pressure, and then the crude product was purified by column chromatography (SiO_2, ethyl acetate: petroleum ether = 1:4 v/v) producing a yellow solid Compound 1 (750 mg, yield: 50.6 %). ^{1}H NMR (400 MHz, Chloroform-*d*) δ 9.88 (s, 1H), 8.65-8.63 (d, J = 8.4 Hz, 1H), 8.09 (s, 1H), 7.87 (s, 1H), 7.84-7.82 (d, J = 8.4 Hz, 1H), 2.31 (s, 3H). ^{13}C NMR (101 MHz, Chloroform-*d*) δ 189.60, 168.46, 140.79, 133.02, 132.78, 130.80, 120.74, 113.12, 25.15; HRMS-ESI (m/z): calcd for $C_9H_8BrNO_2$ [M+H] = 241.9811 / 243.9791; found 241.9812 / 243.9793, [M+Na] = 263.9631 / 265.9611; found 263.9639 / 265.9620.

Synthesis of compound 2 [2]

Compounds 1 (1.205g, 5.0 mmol), (2-(methylthio)phenyl) boronic acid (1.092 g, 6.5 mmol) and tetrakis(triphenylphosphine)palladium (578 mg, 0.5 mmol) were dissolved in toluene (120 mL) under the protection of argon. Potassium carbonate (4 M, 60 mL) and absolute ethanol (16 mL) were added to the reaction solution, and the reaction solution was heated at 80 ℃ for 24 h. After cooling to room temperature, the solvent was removed under reduced pressure, and then the crude product was purified by column chromatography (SiO_2, dichloromethane) producing a brown solid Compound 2 (1.129 g, yield: 79.2 %). ^{1}H NMR (400 MHz, DMSO-d_6) δ 9.94 (s, 1H), 8.88 (s, 1H),

8.13-8.10 (d, J = 8.8 Hz, 1H), 7.90-7.88 (d, J = 8.4 Hz, 1H), 7.69 (s, 1H), 7.48-7.40 (m, 2H), 7.30-7.26 (t, J = 7.2 Hz, 1H), 7.19-7.17 (d, J = 7.6 Hz, 1H), 2.37 (s, 3H), 1.94 (s, 3H). ^{13}C NMR (101 MHz, DMSO-d_6) δ 192.35, 169.42, 142.04, 138.37, 135.75, 133.09, 132.76, 132.36, 130.85, 129.60, 129.43, 126.00, 125.38, 124.09, 24.24, 15.44.

Synthesis of compound 3 [3]

Under the protection of argon, 2-methylquinoline (1.43 g,10 mmol) and iodide ethane (4.68 g, 30 mmol) were dissolved in acetonitrile (20 mL) and heated to reflux for 24 h. After cooling to room temperature, the solvent was removed under reduced pressure to give a yellow solid Compound 3 (1.033 g, yield: 60.0 %). ^{1}H NMR (400 MHz, DMSO-d_6) δ 9.12-9.09 (d, J = 9.2 Hz, 1H), 8.63-8.60(d, J = 9.2 Hz, 1H), 8.43-8.41 (d, J = 8.0 Hz, 1H), 8.26-8.22 (t, J = 8.8 Hz, 1H), 8.14-8.12 (d, J = 8.4 Hz, 1H), 8.02-7.98 (t, J = 8.0 Hz, 1H), 5.03-4.98 (m, 2H), 3.12 (s, 3H), 1.55-1.52 (t, J = 7.6 Hz, 3H). ^{13}C NMR (101 MHz, DMSO-d_6) δ 161.01, 146.11, 138.55, 135.76, 131.12, 129.51, 128.74, 126.04, 119.33, 47.66, 22.84, 13.91. HRMS-ESI (m/z: calcd for $C_{12}H_{14}N^+$ [M+H] = 173.1199; found 173.1170.

Synthesis of compound 4 [4]

Compound 3 (2.2 g, 12.78 mmol) and malononitrile (1.81 g, 27.36 mmol) were dissolved in absolute ethanol (20 mL). The reaction solution was stirred at 0 ℃ at a constant temperature, and sodium ethanol (1.86 g, 27.36 mmol) was added to the solution. After 4 h of reaction, the reaction mixture was poured into 500 mL ice water and adjusted to pH= 7-8 with 1 M hydrochloric acid solution. The precipitated solid was filtered and wash with water. Then the solid was dried and yellow solid compound 4 was obtained (716 mg, yield: 23.8 %). ^{1}H NMR (400 MHz, Chloroform-d) δ 9.11-9.09 (d, J = 8.4 Hz, 1H), 7.77-7.73 (t, J = 8.8 Hz, 1H), 7.62-7.60 (d, J = 7.6 Hz, 1H), 7.46-7.42 (t, J = 8.4 Hz, 1H), 6.82 (s, 1H), 4.36-4.31 (m, 2H), 2.59 (s, 3H), 1.51-1.47 (t, J = 7.2 Hz, 3H). ^{13}C NMR (101 MHz, Chloroform-d) δ 148.81, 142.68, 133.36, 128.40, 122.22, 119.83, 116.77, 115.45, 114.27, 111.28, 105.19, 45.73, 38.12, 16.77, 8.99. HRMS-ESI (m/z): calcd for $C_{15}H_{13}N_3$ [M+H] = 236.1182; found 236.1191,

[M+Na] = 258.1002; found 258.1019.

Synthesis of compound 5 [4]

Compound 2 (57 mg, 0.20 mmol) and 4 (39.3 mg, 0.167 mmol) were dissolved in acetonitrile (10 mL), piperidine (0.2 mL) was added, and heated to reflux for 6 h under the protection of argon. After cooling to room temperature, the solvent was removed under reduced pressure, and then the crude product was purified by column chromatography (SiO_2, dichloromethane: ethyl acetate = 10:1 v/v) producing the orange solid Compound 5 (42 mg, yield: 50.1 %). ^{1}H NMR (400 MHz, DMSO-d_6) δ 8.94-8.92 (d, J = 8.4 Hz, 1H), 8.70 (s, 1H), 8.10-8.07 (d, J = 8.8 Hz, 1H), 7.94-7.81 (m, 3H), 7.64-7.59 (m, 2H), 7.45-7.39 (m, 3H), 7.29-7.25 (t, J = 7.6 Hz, 1H), 7.20-7.18 (d, J = 7.6 Hz, 1H), 7.02 (s, 1H), 4.60-4.55 (m, 2H), 2.38 (s, 3H), 1.90 (s, 3H), 1.40-1.37 (t, J = 7.2 Hz, 3H). ^{13}C NMR (101 MHz, DMSO-d_6) δ 169.11, 152.77, 149.90, 139.64, 138.41, 138.30, 137.84, 136.50, 134.22, 131.09, 130.89, 129.12, 128.20, 125.75, 125.62, 125.49, 125.15, 121.12, 120.57, 118.65, 107.51, 55.40, 47.38, 44.30, 15.47, 14.17. HRMS-ESI (m/z): calcd for $C_{31}H_{26}N_4SO$ [M+H] = 503.1900; found 503.1977, [M+Na] = 525.1720; found 525.1805.

Synthesis of QM-S [5]

Hydrochloric acid: absolute ethanol = 1:10 (22 mL in total) was added to a single-mouth round-bottom flask containing compound 7 (75 mg, 0.15 mmol), and heated to reflux for 6 h. After cooling to room temperature, dichloromethane was used to extract the resulted mixture and the combined organic phase was concentrated under reduced pressure. Then the crude product was purified by column chromatography (SiO_2, dichloromethane) producing the yellow solid product QM-S (16 mg, yield: 23.2 %). ^{1}H NMR (400 MHz, DMSO-d_6) δ 8.93-8.90 (d, J = 8.8 Hz, 1H), 8.07-8.05 (d, J = 8.8 Hz, 1H), 7.92-7.88 (t, J = 8.8 Hz, 1H), 7.61-7.57 (t, J = 8.4 Hz, 2H), 7.44-7.32 (m, 4H), 7.27-7.15 (m, 3H), 7.03 (s, 1H), 6.82-6.80 (d, J = 8.8 Hz, 1H), 5.13 (s, 2H), 4.58-4.53 (m, 2H), 2.38 (s, 3H), 1.40-1.36 (t, J = 7.2 Hz, 3H). ^{13}C NMR (101 MHz, DMSO-d_6) δ 152.23, 150.55, 148.43, 141.43, 138.88, 138.37, 136.75, 133.94, 131.57, 130.73,

129.92, 128.96, 125.56, 125.31, 125.24, 125.21, 124.67, 123.63, 121.12, 118.52, 115.18, 114.57, 106.65, 46.11, 44.00, 15.02, 14.15. HRMS-ESI (m/z): calcd for $C_{29}H_{24}N_4S$ [M+H] = 461.1794; found 461.1829, [M+Na] = 483.1614; found 483.1652. [M+K] = 499.1353; found 499.1393.

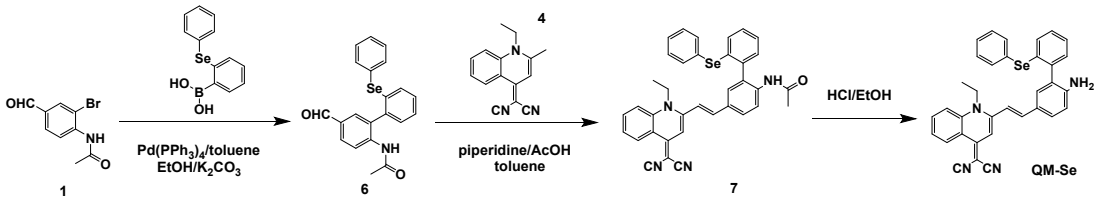

Fig. S2 Synthesis procedure of QM-Se.

Synthesis of compound 6 [2]

Compounds 1 (241 mg, 1.0 mmol), (2-(phenylselanyl)phenyl) boronic acid (361.4 mg, 1.3 mmol) and tetrakis(triphenylphosphine)palladium (115.6 mg, 0.1 mmol) were dissolved in toluene (24 mL) under the protection of argon. Potassium carbonate (4 M, 12 mL) and absolute ethanol (3.2 mL) were added to the reaction solution, and the reaction solution was heated at 80 ℃ for 24 h. After cooling to room temperature, the solvent was removed under reduced pressure, and then the crude product was purified by column chromatography (SiO_2, dichloromethane) producing a brown solid Compound 6 (300 mg, yield: 75.9 %). 1H NMR (400 MHz, Chloroform-d) δ 9.82 (s, 1H), 8.57-8.55 (d, J = 8.4 Hz, 1H), 7.88-7.85 (d, J = 10.4 Hz, 1H), 7.58 (s, 1H), 7.40-7.34 (m, 4H), 7.31-7.16 (m, 6H), 1.99 (s, 3H). 13C NMR (101 MHz, Chloroform-*d*) δ 190.89, 189.58, 168.35, 140.69, 137.35, 134.93, 134.04, 132.59, 131.89, 131.72, 130.91, 130.87, 129.80, 129.55, 128.96, 128.42, 127.82, 120.26, 24.91. HRMS-ESI (m/z): calcd for $C_{21}H_{17}O_2NSe$ [M+Na] = 418.0318; found 418.0335.

Synthesis of compound 7 [4]

Compound 6 (24.8 mg, 0.105 mmol) and 4 (50 mg, 0.127 mmol) were dissolved in acetonitrile (10 mL), piperidine (0.2 mL) was added, and heated to reflux for 6 h under the protection of argon. After cooling to room temperature, the solvent was removed under reduced pressure, and then the crude product was purified by column

chromatography (SiO_2, dichloromethane: ethyl acetate = 50:1 v/v) producing the orange solid Compound 7 (36 mg, yield: 56.0 %). ^{1}H NMR (400 MHz, DMSO-d_6) δ 8.95-8.90 (m, 2H), 8.10-8.08 (d, J = 8.8 Hz, 1H), 7.95-7.81 (m, 3H), 7.64-7.57 (m, 2H), 7.50-7.30 (m, 5H), 7.36-7.30 (m, 6H), 7.02 (s, 1H), 4.59-4.54 (m, 2H), 1.92 (s, 3H), 1.40-1.36 (t, J = 7.2 Hz, 3H). ^{13}C NMR (101 MHz, DMSO-d_6) δ 152.79, 149.83, 140.24, 139.55, 138.14, 137.65, 134.19, 132.83, 131.56, 130.84, 130.74, 130.06, 129.34, 128.31, 127.90, 125.64, 125.48, 121.12, 120.56, 118.64, 107.47, 47.44, 44.30, 24.04, 14.17. HRMS-ESI (m/z): calcd for $C_{36}H_{28}ON_4Se$ [M+Na] = 635.1323; found 635.1334.

Synthesis of QM-Se [5]

Hydrochloric acid: absolute ethanol = 1:10 (11mL in total) was added to a single-mouth round-bottom flask containing compound 5 (21 mg, 0.034 mmol), and heated to reflux for 6 h. After cooling to room temperature, dichloromethane was used to extract the resulted mixture and the combined organic phase was concentrated under reduced pressure. Then the crude product was purified by column chromatography (SiO_2, dichloromethane: ethyl acetate = 100:1 v/v) producing the dark red solid product QM-Se (5.8 mg, yield: 29.9 %). ^{1}H NMR (400 MHz, DMSO-d_6) δ 8.93-8.90 (d, J = 8.4 Hz, 1H), 8.07-8.05 (d, J = 8.8 Hz, 1H), 7.93-7.88 (m, 1H), 7.61-7.48 (m, 4H), 7.38-7.17 (m, 9H), 7.03 (s, 1H), 6.84-6.82 (d, J = 8.4 Hz, 1H), 5.76 (s, 1H), 5.29 (s, 2H), 4.58-4.53 (m, 2H), 1.41-1.37 (t, J = 7.2 Hz, 3H). ^{13}C NMR (101 MHz, DMSO-d_6) δ 152.24, 150.50, 148.36, 141.36, 139.99, 138.39, 134.86, 133.94, 131.86, 131.33, 131.26, 130.13, 129.23, 128.54, 127.84, 125.73, 125.57, 125.21, 123.51, 121.12, 118.52, 115.23, 114.59, 106.60, 55.39, 46.12, 44.00, 14.17. HR-ESI (m/z): calcd for $C_{34}H_{26}N_4Se$ [M+H] = 571.1398; found 571.1454, [M+Na] = 593.1217; found 593.1250.

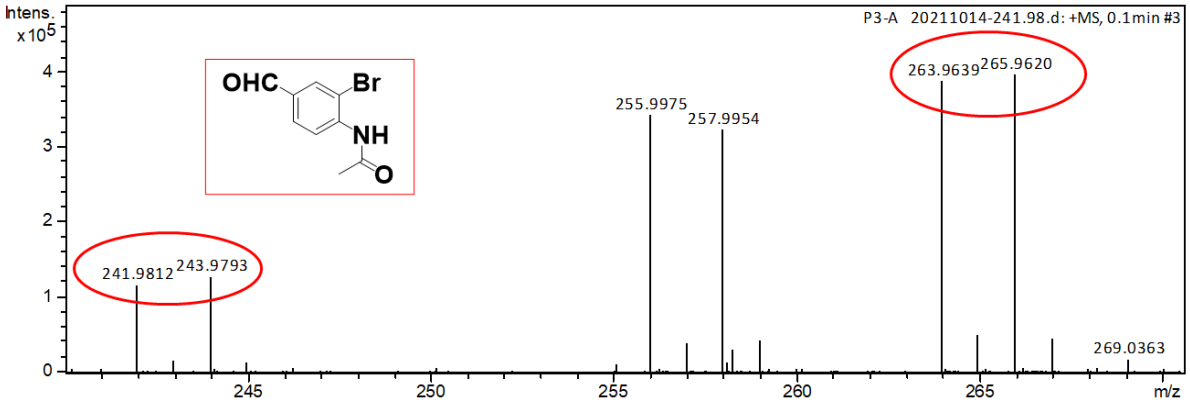

Fig. S3 HRMS of compound 1.

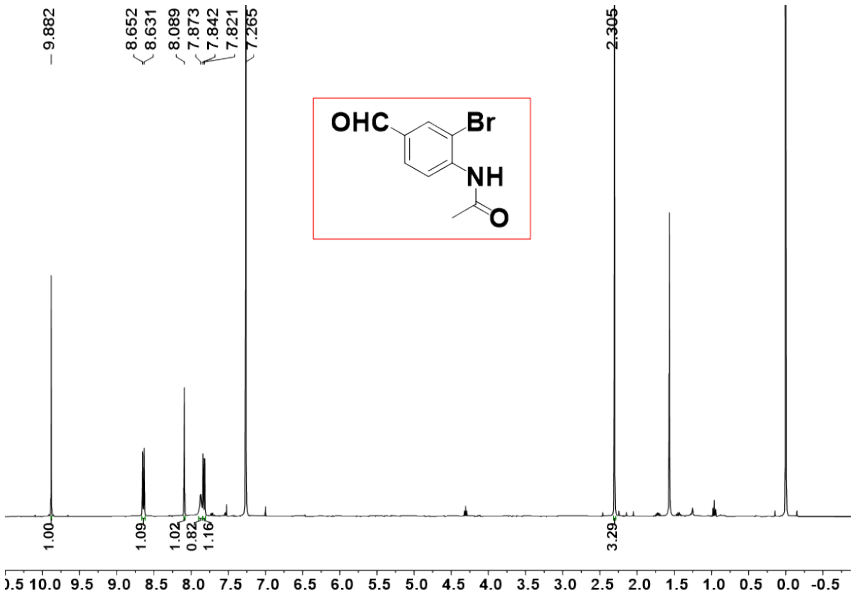

Fig. S4 ^{1}H NMR spectrum of compound 1 in $CDCl_3$.

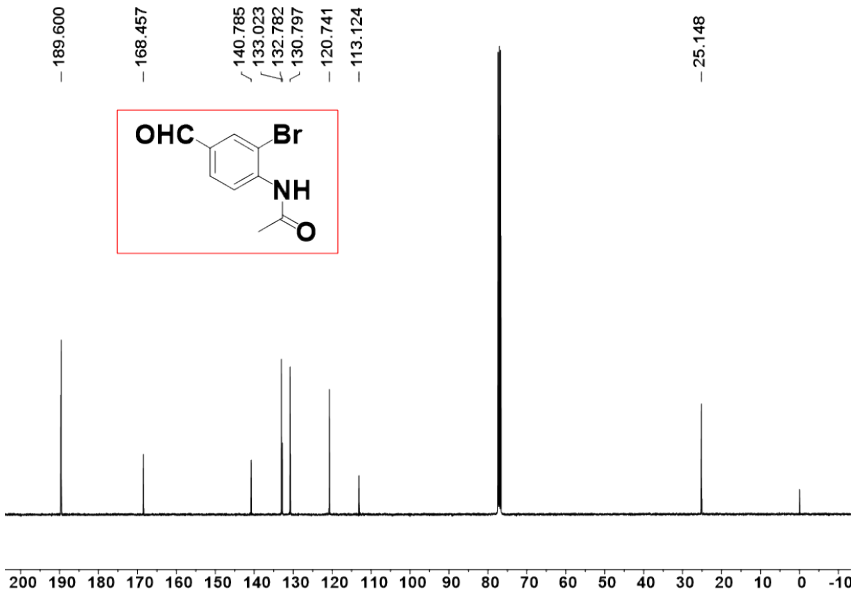

Fig. S5 ^{13}C NMR spectrum of compound 1 in $CDCl_3$.

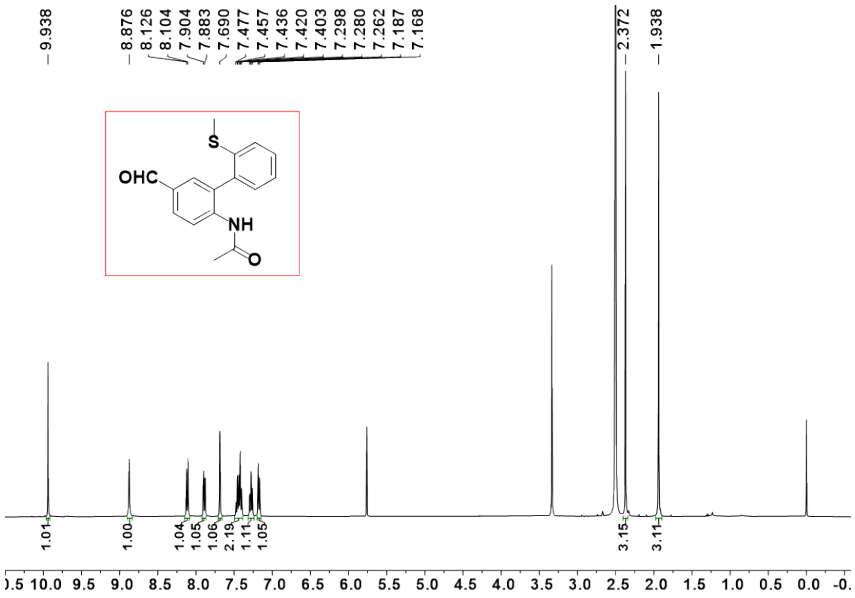

Fig. S6 ^{1}H NMR of compound 2.

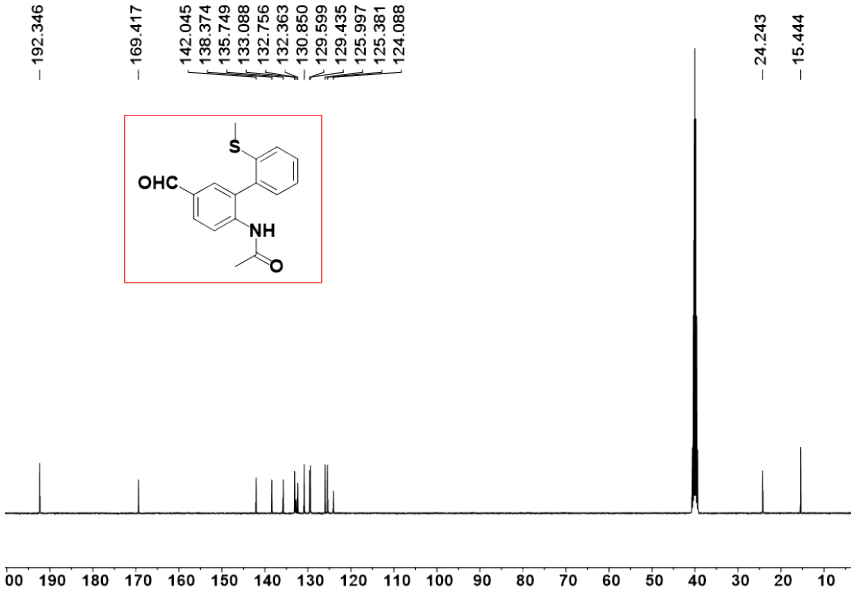

Fig. S7 ^{13}C NMR spectrum of compound 2 in $CDCl_3$.

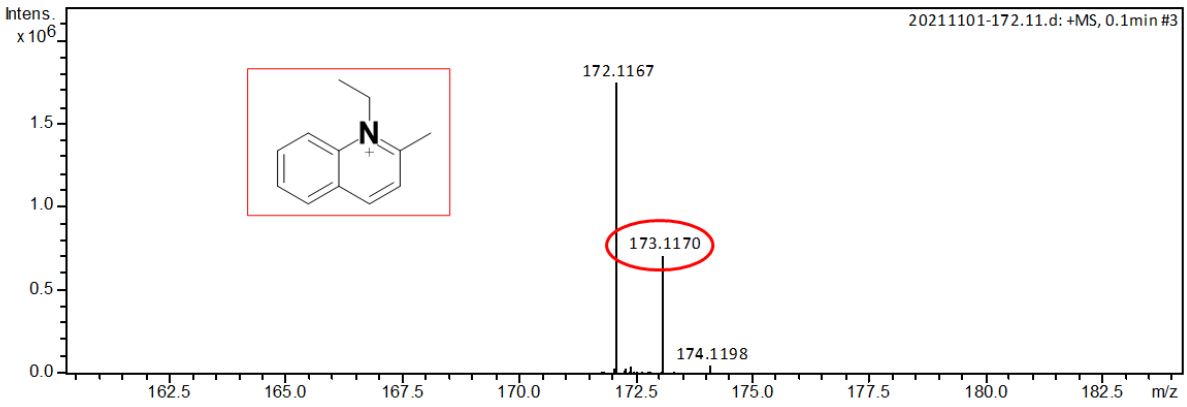

Fig. S8 HRMS of compound 3.

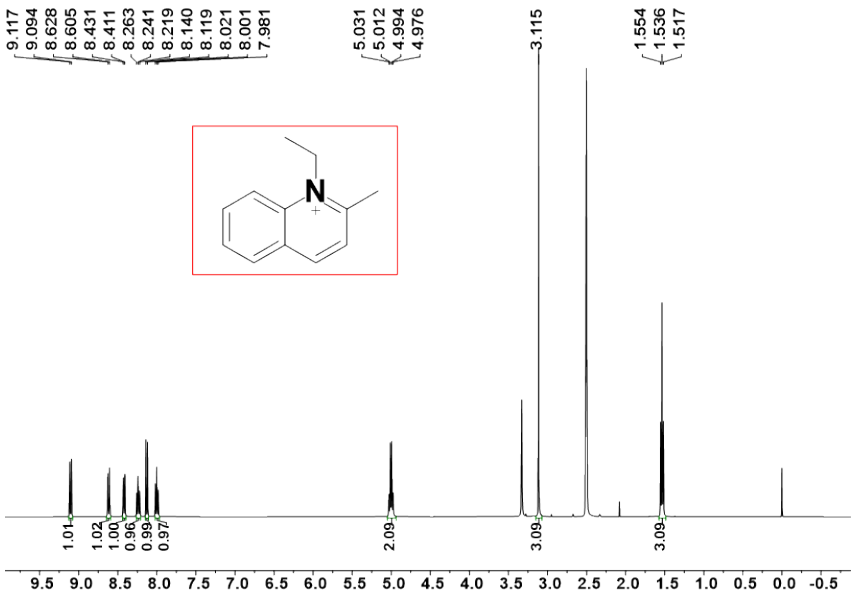

Fig. S9 ^{1}H NMR spectrum of compound 3 in $CDCl_3$.

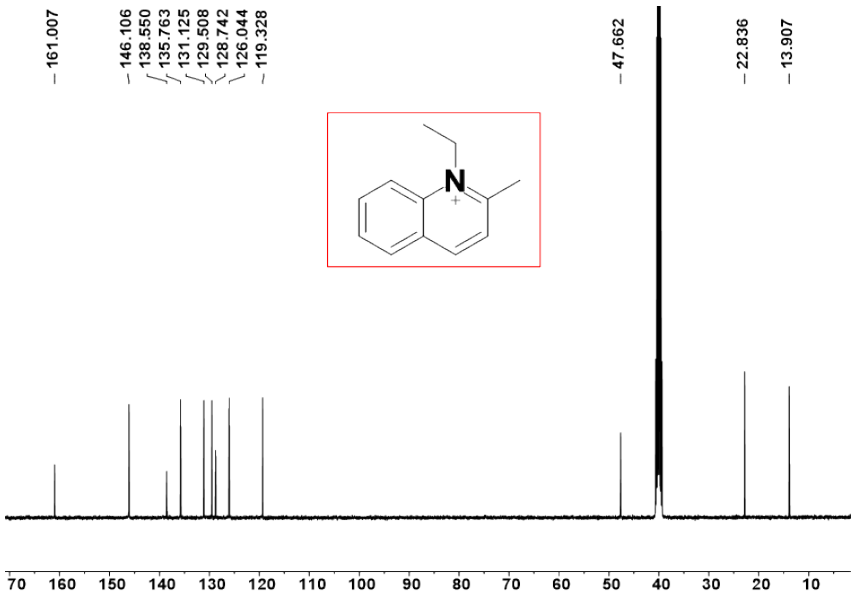

Fig. S10 ^{13}C NMR spectrum of compound 3 in $CDCl_3$.

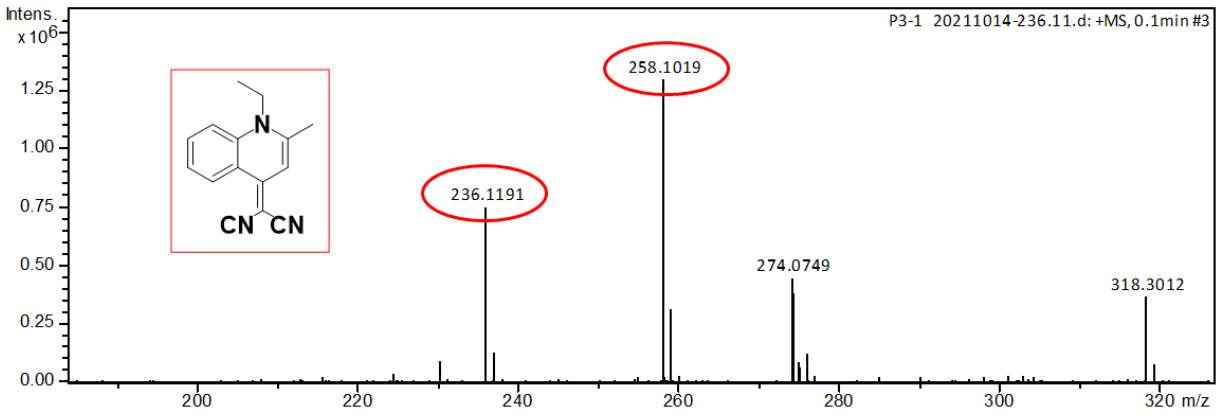

Fig. S11 HRMS of compound 4.

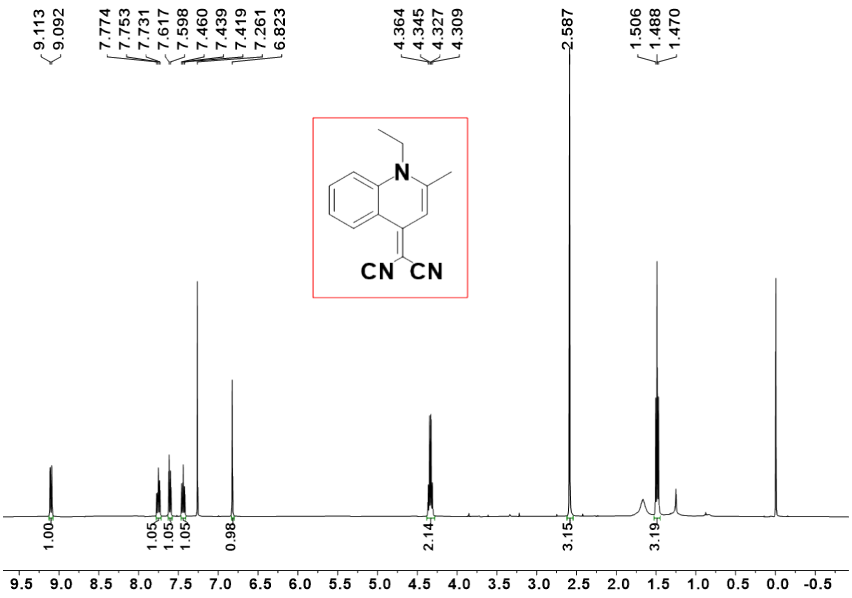

Fig. S12 ^{1}H NMR spectrum of compound 4 in $CDCl_3$.

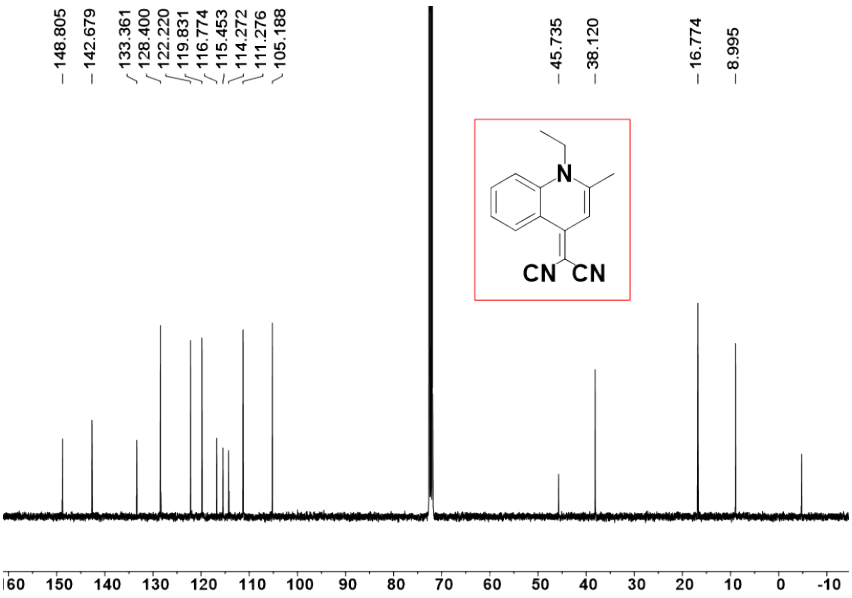

Fig. S13 ^{13}C NMR spectrum of compound 4 in $CDCl_3$.

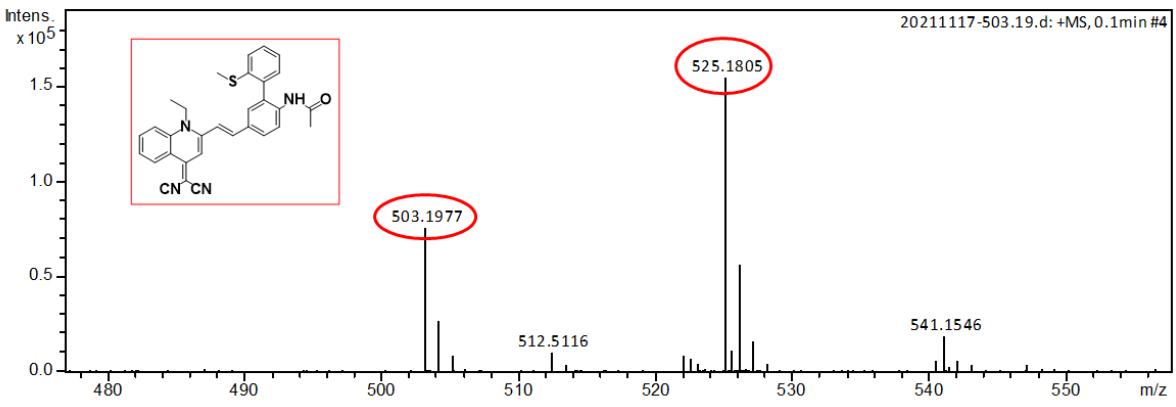

Fig. S14 HRMS of compound 5.

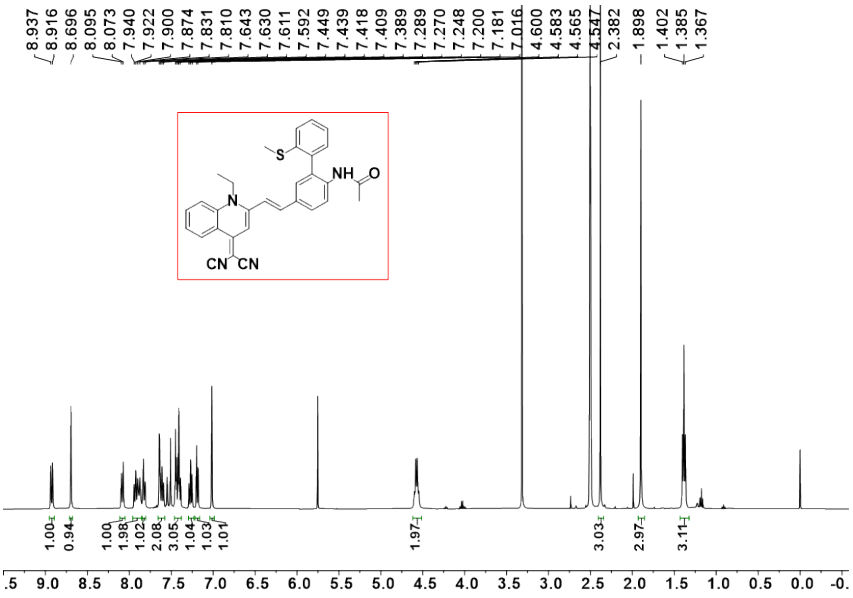

Fig. S15 ^{1}H NMR spectrum of compound 5 in $CDCl_3$.

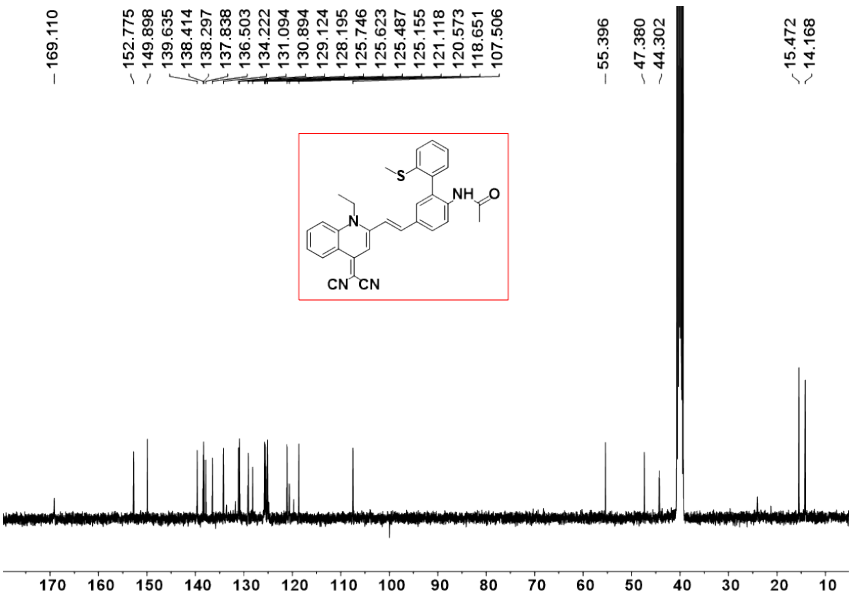

Fig. S16 ^{13}C NMR spectrum of compound 5 in $CDCl_3$.

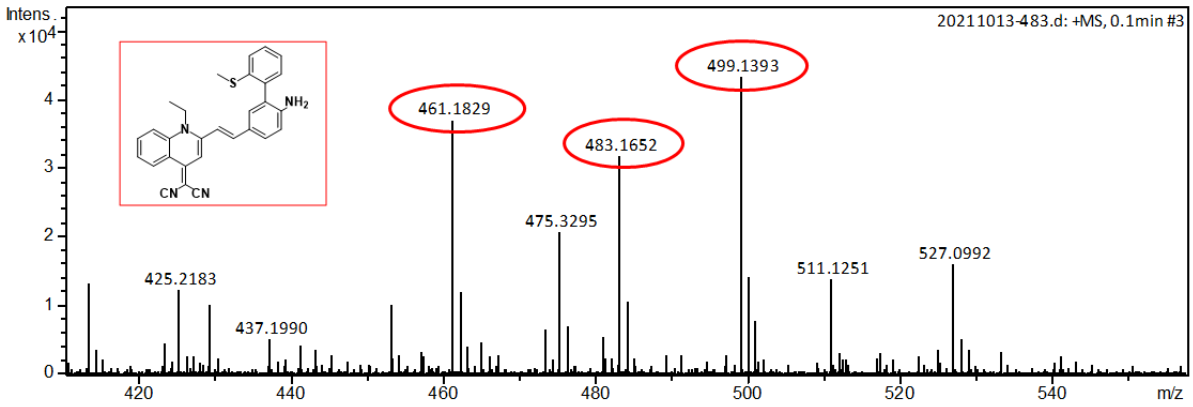

Fig. S17 HRMS of QM-S.

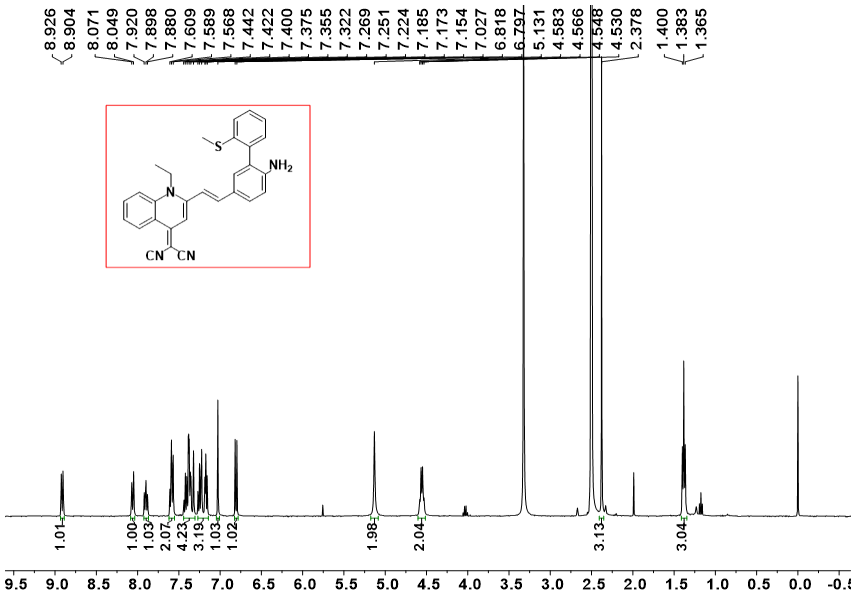

Fig. S18 ^{1}H NMR spectrum of QM-S in $CDCl_3$.

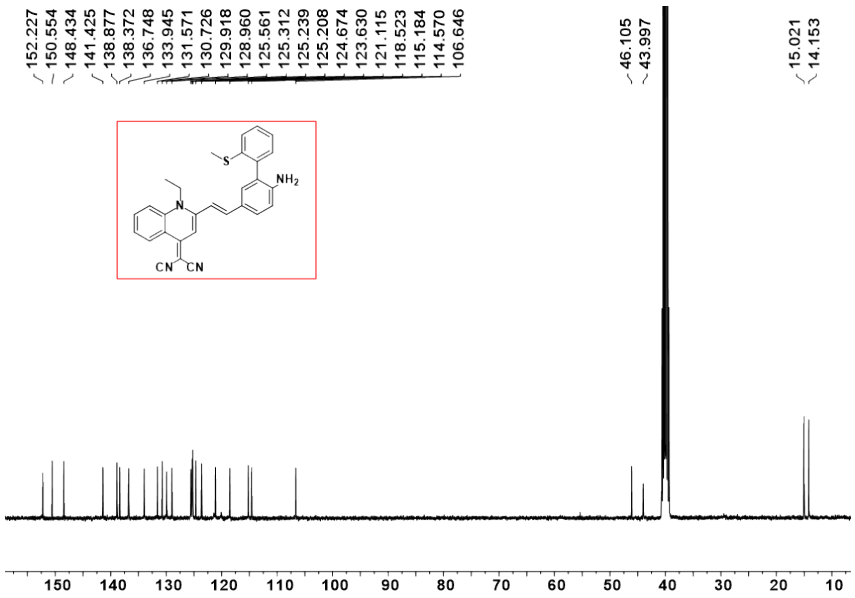

Fig. S19 ^{13}C NMR spectrum of QM-S in $CDCl_3$.

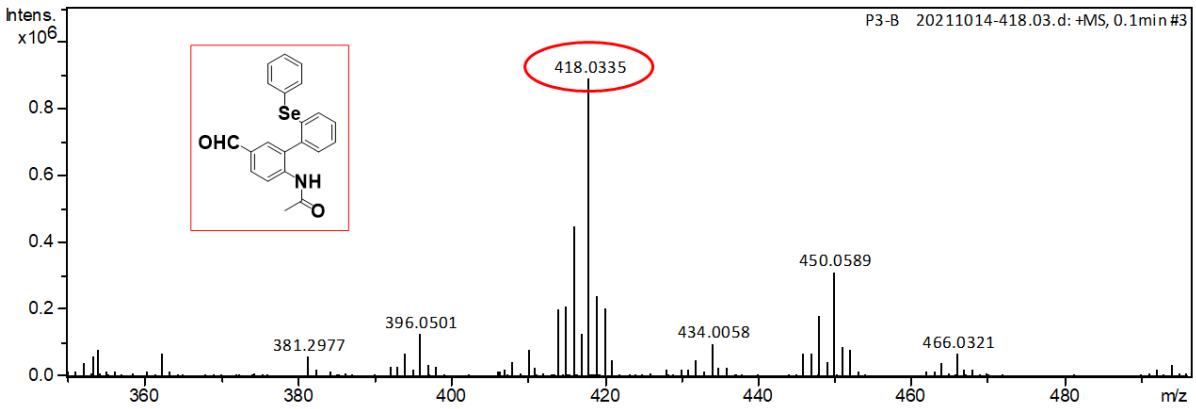

Fig. S20 HRMS of compound 6.

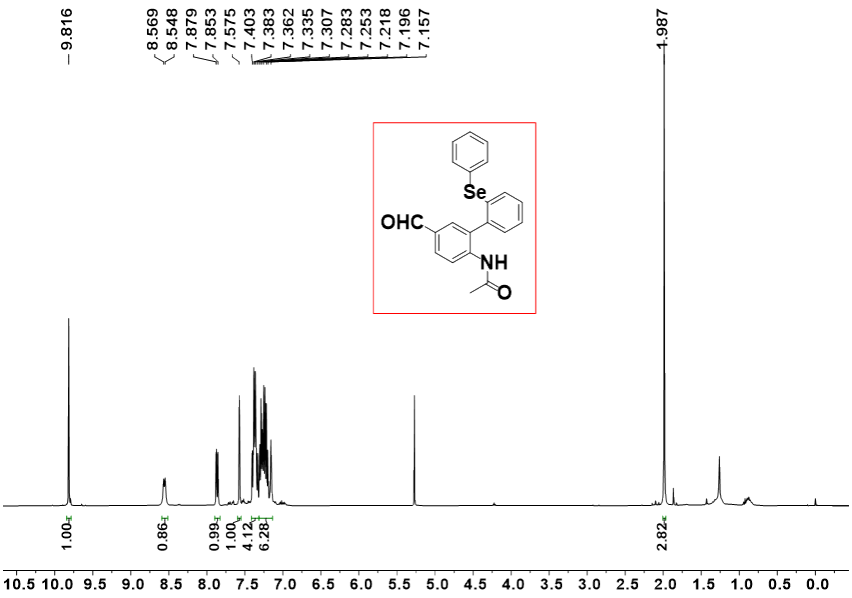

Fig. S21 ^{1}H NMR spectrum of compound 6 in $CDCl_3$.

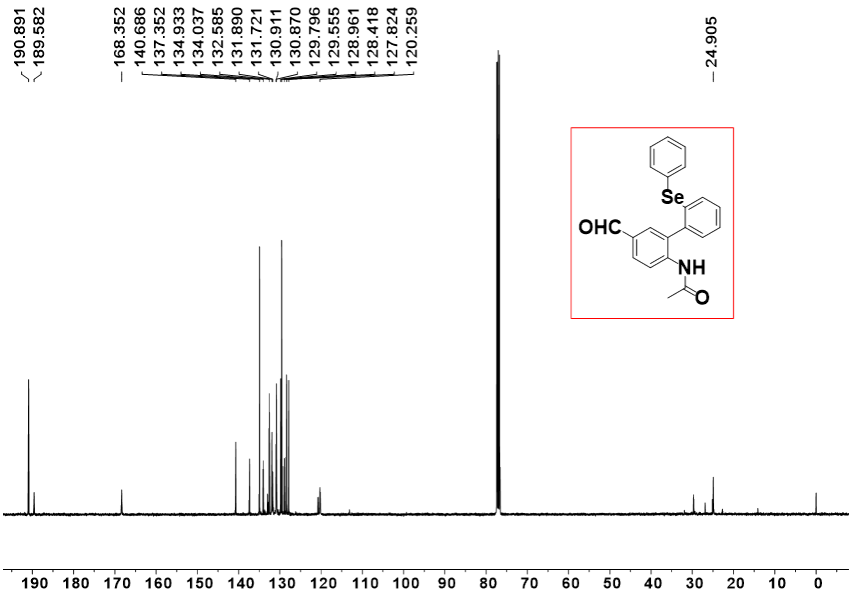

Fig. S22 ^{13}C NMR spectrum of compound 6 in $CDCl_3$.

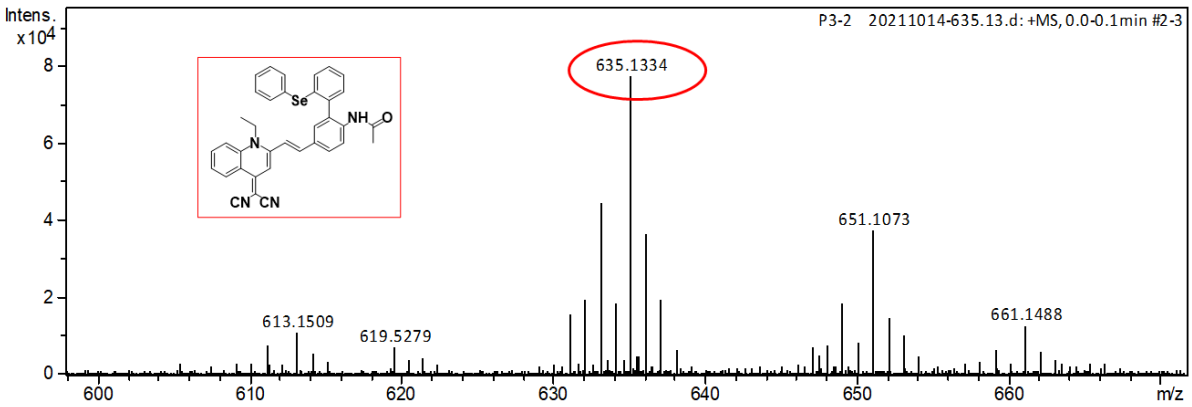

Fig. S23 HRMS of compound 7.

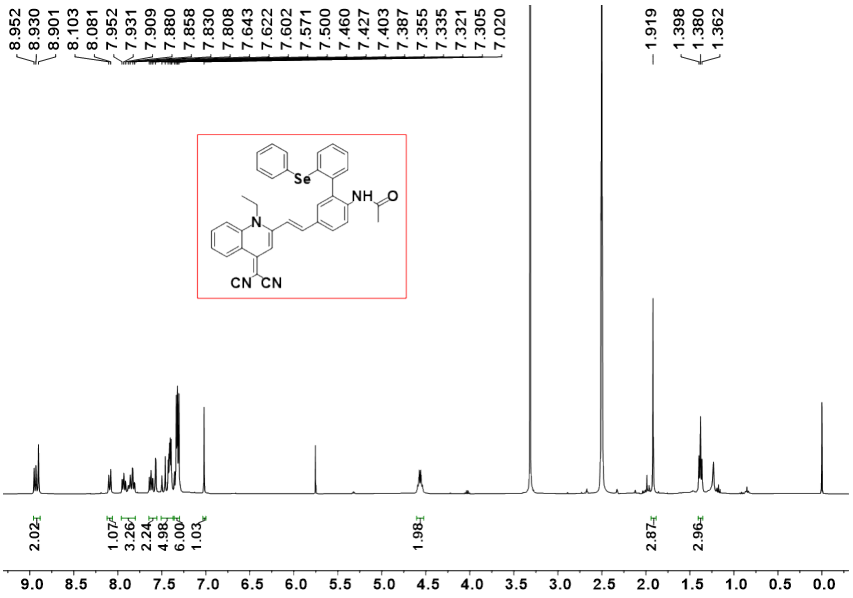

Fig. S24 ^{1}H NMR spectrum of compound 7 in $CDCl_3$.

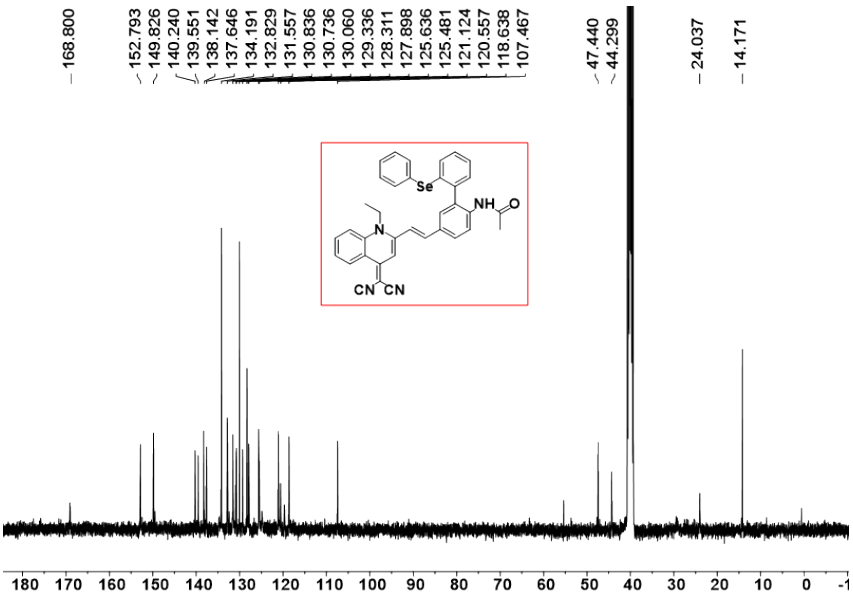

Fig. S25 13C NMR spectrum of compound 7 in $CDCl_3$.

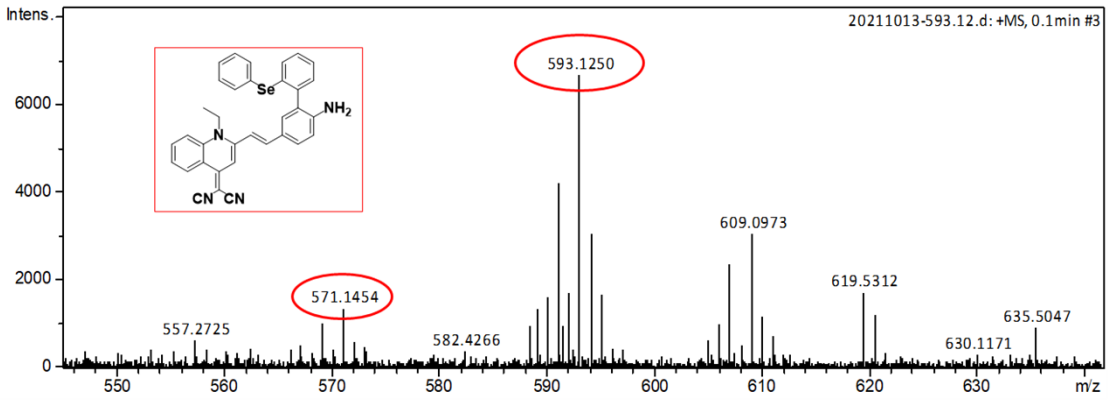

Fig. S26 HRMS of compound QM-Se.

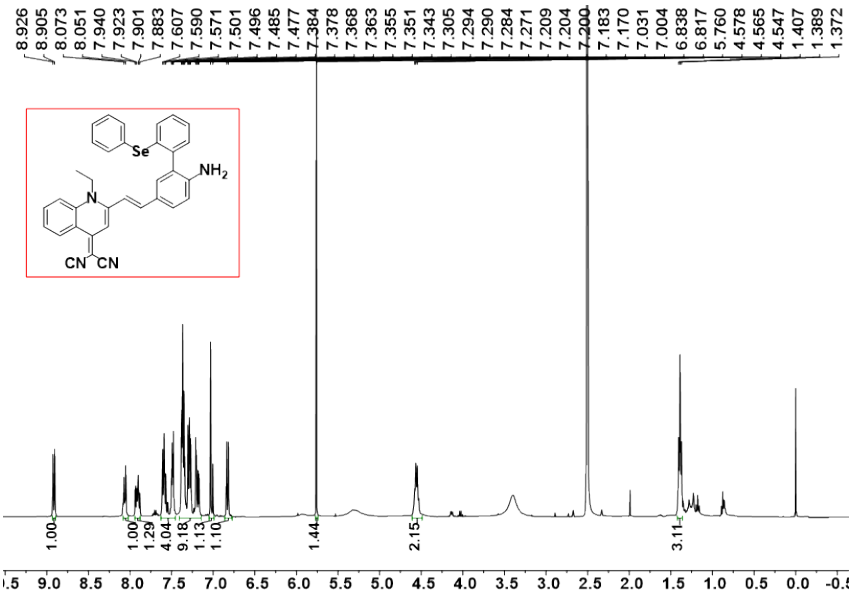

Fig. S27 ^{1}H NMR spectrum of QM-Se in $CDCl_3$.

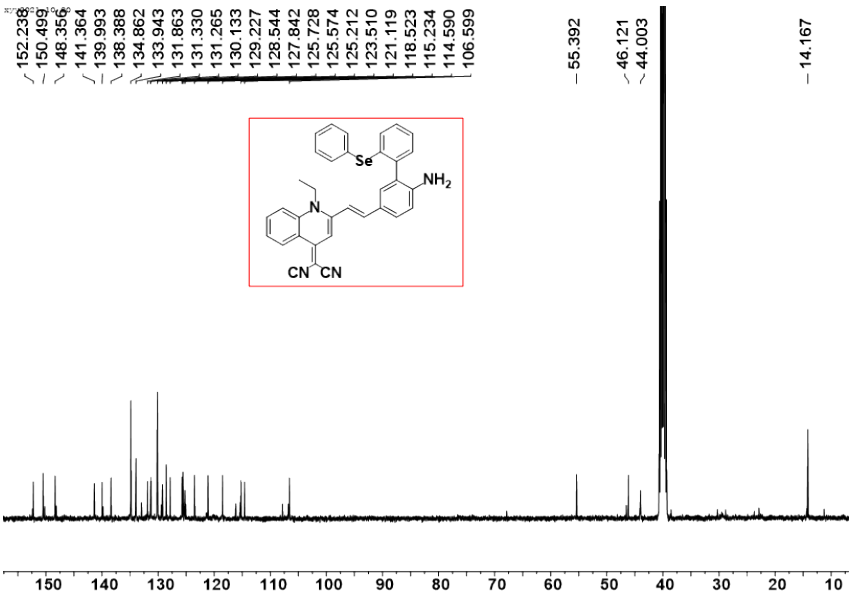

Fig. S28 ^{13}C NMR spectrum of QM-Se in $CDCl_3$.

4. Preparation of QM-S NPs/ QM-Se NPs

Under ultrasound, the THF/DMSO solution of QM-S was added to deionized water, respectively, then shaken vigorously to afford QM-S NPs. QM-Se NPs were prepared in the same way.

5. Cell culture

The H9C2 cell lines were grown in Dulbecco's modified Eagle's medium (DMEM) with 1 % 100 U mL^{-1} antibiotics penicillin/streptomycin and 10 % fetal bovine serum (FBS) at 37 °C under a humidified atmosphere containing 5 % CO_2.

6. MTT assay

The cytotoxicity of the probe was tested in H9C2 cells using a standard MTT assay. The IC_{50} value was calculated according to the method of Huber and Koella[2]. It was displayed that the value of IC_{50} was 267.8 μM for QM-S and 236.0 μM for QM-Se respectively, which indicated the good biocompatibility for cell imaging.

7. Cell imaging

H9C2 cells were employed to perform the imaging.

One-photon confocal fluorescent imaging of exogenous HOBr in H9C2 cells with QM-S/QN-Se

The cells were washed with PBS for three times firstly. Group a: H9C2 cells were incubated with PBS alone for 15 min, the PBS was washed away and the imaging was carried out. Group b: H9C2 cells were incubated with QM-S/QM-Se (5.0 μM) alone for 15 min, the QM-S/QM-Se solution was washed away and the imaging was carried out. Group c: H9C2 cells were pretreated with HOBr (50.0 μM) for 10 min and washed with PBS for three times; After culturing with QM-S/QM-Se (5.0 μM) for 15 min, the QM-S/QM-Se solution was washed away and the imaging was carried out. Group d: H9C2 cells were pretreated with KBr (100.0 μM) and HOBr (50.0 μM) for 20 min and washed with PBS for three times; After culturing with QM-S/QM-Se (5.0 μM) for 15 min, the QM-S/QM-Se solution was washed away and the imaging was carried out. QM-S: $\lambda_{ex}/\lambda_{em}$=405 nm/550-645 nm; QM-Se: $\lambda_{ex}/\lambda_{em}$=405 nm/550-650 nm.

One-photon confocal fluorescent imaging of endogenous HOBr in H9C2 cells with QM-S/QN-Se

The cells were washed with PBS for three times firstly. Group a: H9C2 cells were incubated with QM-S/QM-Se (5.0 μM) alone for 15 min, after washing away QM-S/QM-Se solution, PBS was added again to image as control group. Group b: H9C2 cells were pretreated with KBr (100.0 μM) for 20 min and washed with PBS for three times; After culturing with QM-S/QM-Se (5.0 μM) for 15 min, the QM-S/QM-Se solution was washed away and the imaging was carried out. Group c: H9C2 cells were successively pretreated with dapsone (15.0 μM, 20 min) and KBr (100.0 μM, 20 min) and washed with PBS for three times; After culturing with QM-S/QM-Se (5.0 μM) for 15 min, the QM-S/QM-Se solution was washed away and the imaging was carried out. Group d: H9C2 cells were pretreated with KBr (100.0 μM) and H_2O_2 (100.0 μM) for 20 min and washed with PBS for three times; After culturing with QM-S/QM-Se (5.0 μM) for 15 min, the QM-S/QM-Se solution was washed away and the imaging was carried out. Group e: H9C2 cells were pretreated with dapsone (15.0 μM) for 20 min and washed with PBS for three times, then treated with KBr (100.0 μM) and H_2O_2 (100.0 μM) for 20 min and washed with PBS for three times; After culturing with QM-S/QM-Se (5.0 μM) for 15 min, the QM-S/QM-Se solution was removed and the imaging was carried out. Group f: H9C2 cells were pretreated with KBr (100.0 μM) and NAC (100.0 μM) for 20 min and washed with PBS for three times; After culturing with QM-S/QM-Se (5.0 μM) for 15 min, the QM-S/QM-Se solution was washed away and the imaging was carried out. QM-S: $\lambda_{ex}/\lambda_{em}$=405 nm/550-645 nm; QM-Se: $\lambda_{ex}/\lambda_{em}$=405 nm/550-650 nm.

Establishment of OGD/R

H9C2 cells were cultured under normoxic conditions (37%, 5%CO_2) for 24 h. H9C2 cells were washed three times with PBS and then cultured with DMEM without glucose for 10 min to remove residual oxygen. The dishes were placed into an airtight AnaeroPouch bag, which provided near anaerobic conditions with an O_2 concentration <1% (monitored with the oxygen indicator) and a CO_2 concentration of about 5% within 1 h of incubation at 37 °C. Cells were exposed to these conditions for 5 h. After this, the cells were washed with PBS three times, and then incubated again in high-glucose DMEM at 37 °C in 95% air/5% CO_2 for another 1 h.

One-photon confocal fluorescent imaging of HOBr in H9C2 cells with QM-S/QN-Se during OGD/R

Confocal imaging during Oxygen-Glucose Deprivation/Reperfusion (OGD/R). Group a: H9C2 cells were incubated with QM-S/QM-Se (5.0 μM) alone for 15 min, after washing away QM-S/QM-Se solution, PBS was added again to image as control group. Group b: The OGD/R H9C2 cells were incubated with QM-S/QM-Se (5.0 μM) for 15 min, the QM-S/QM-Se solution was washed away and the imaging was carried out. Group c: The OGD/R H9C2 cells were pretreated with NAC (100.0 μM) for 20 min and washed with PBS for three times; After culturing with QM-S/QM-Se (5.0 μM) for 15 min, the QM-S/QM-Se solution was washed away and the imaging was carried out. Group d: The OGD/R H9C2 cells were pretreated with dapsone (15.0 μM) for 20 min and washed with PBS for three times; After culturing with QM-S/QM-Se (5.0 μM) for 15 min, the QM-S/QM-Se solution was washed away and the imaging was carried out. QM-S: $\lambda_{ex}/\lambda_{em}$=405 nm/550-645 nm; QM-Se: $\lambda_{ex}/\lambda_{em}$=405 nm/550-650 nm.

Protective effect of estradiol (E2) on H9C2 cells during OGD/R

Group a: H9C2 cells were incubated with QM-S/QM-Se (5.0 μM) alone for 15 min, after washing away QM-S/QM-Se solution, PBS was added again to image as control group. Group b: The OGD/R H9C2 cells were incubated with QM-S/QM-Se (5.0 μM) for 15 min, the QM-S/QM-Se solution was washed away and the imaging was carried out. Group c: H9C2 cells were incubated with E2 (10.0 nM) for 5 h during OGD/R, After culturing with QM-S/QM-Se (5.0 μM) for 15 min, the QM-S/QM-Se solution was washed away and the imaging was carried out. Group d: H9C2 cells were incubated with E2 (10.0 nM) and Fulvestrant (100.0 nM) for 5 h during OGD/R, After culturing with QM-S/QM-Se (5.0 μM) for 15 min, the QM-S/QM-Se solution was washed away and the imaging was carried out. Group e: H9C2 cells were incubated with E2 (10.0 nM) and PPG (100.0 nM) for 5 h during OGD/R, After culturing with QM-S/QM-Se (5.0 μM) for 15 min, the QM-S/QM-Se solution was washed away and the imaging was carried out. QM-S: $\lambda_{ex}/\lambda_{em}$=405 nm/550-645 nm; QM-Se: $\lambda_{ex}/\lambda_{em}$=405 nm/550-650 nm.

Protective effect of drugs on H9C2 cells during OGD/R

Group a: H9C2 cells were incubated with QM-S/QM-Se (5.0 μM) alone for 15 min, after removing QM-S/QM-Se solution, PBS was added again to image as control group. Group b: The OGD/R H9C2 cells were incubated with QM-S/QM-Se (5.0 μM) for 15 min, the QM-S/QM-Se solution was washed away and the imaging was carried out. Group c: H9C2 cells were pretreated with Sulindac (10.0 μM) for 2 h and OGD/R model was established, after culturing with QM-S/QM-Se (5.0 μM) for 15 min, the QM-S/QM-Se solution was washed away and the imaging was carried out. Group d: H9C2 cells were pretreated with Indomethacin (10.0 μM) for 2 h and OGD/R model was established, after culturing with QM-S/QM-Se (5.0 μM) for 15 min, the QM-S/QM-Se solution was washed away and the imaging was carried out. Group e: H9C2 cells were pretreated with Ferrostatin-1 (10.0 μM) for 2 h and OGD/R model was established, after culturing with QM-S/QM-Se (5.0 μM) for 15 min, the QM-S/QM-Se solution was washed away and the imaging was carried out. QM-S: $\lambda_{ex}/\lambda_{em}$=405 nm/550-645 nm; QM-Se: $\lambda_{ex}/\lambda_{em}$=405 nm/550-650 nm.

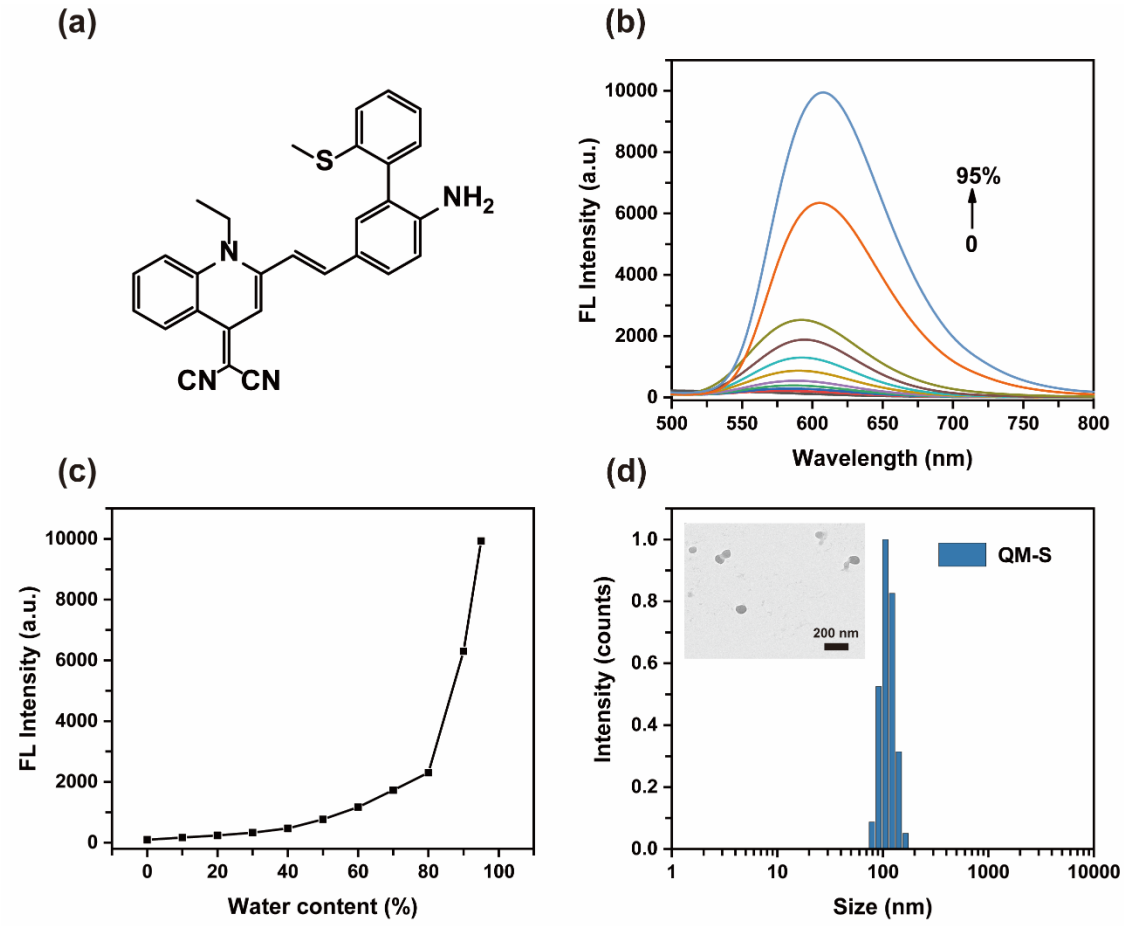

Fig. S29 (a) The molecular structure of QM-S. (b) Fluorescent intensity of QM-S (10 μM) in water/THF mixtures with different water fraction (λex =420 nm). (c) Plot of fluorescence intensity of QM-S (measured at 610 nm) in water/THF mixtures with different water fraction. (d) DLS and TEM (inset) photograph of QM-S NPs.

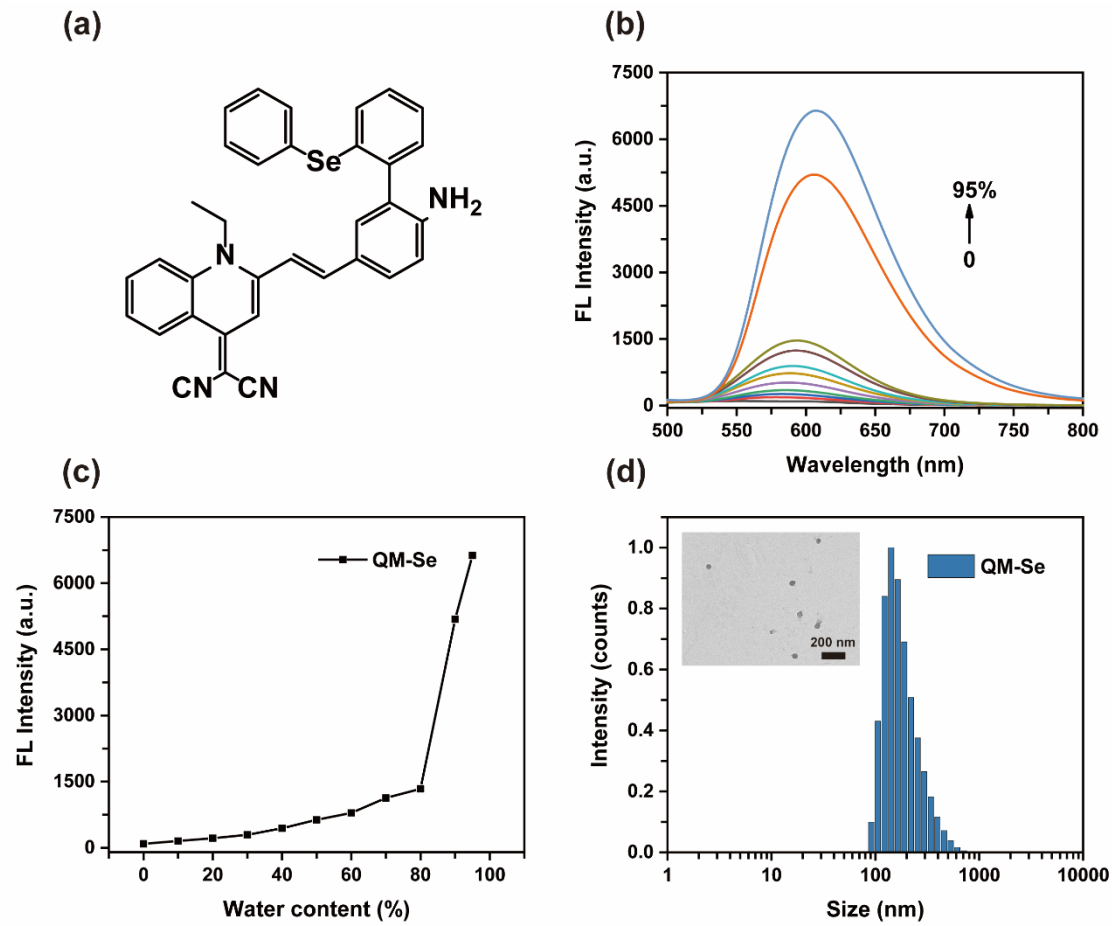

Fig. S30 (a) The molecular structure of QM-Se. (b) Fluorescent intensity of QM-Se (10 μM) in water/THF mixtures with different water fraction (λ_{ex} =420 nm). (c) Plot of fluorescence intensity of QM-Se (measured at 610 nm) in water/THF mixtures with different water fraction. (d) DLS and TEM (inset) photograph of QM-Se NPs.

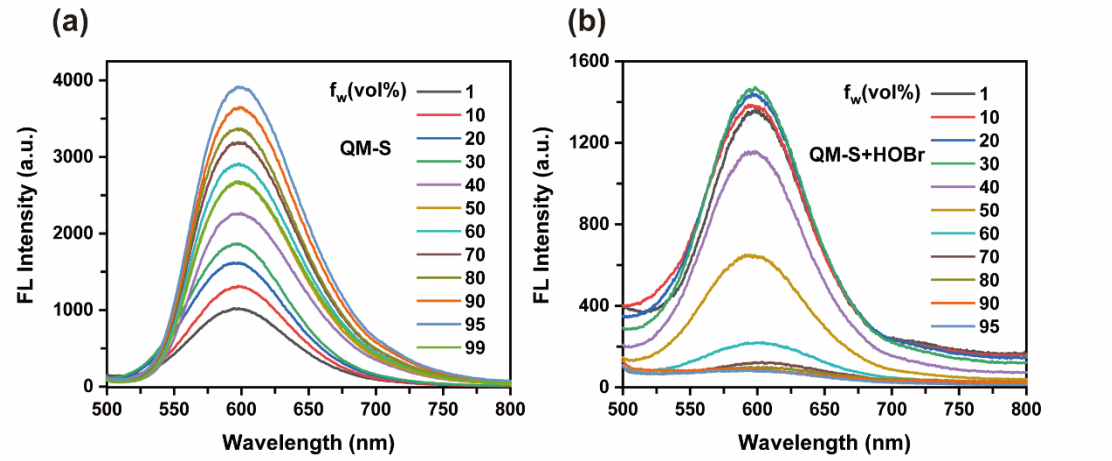

Fig. S31 (a) Fluorescent intensity of QM-S (10 μM) in water/DMSO mixtures with different water fraction (λ_{ex} =420 nm). (b) Fluorescent intensity of QM-S (10 μM) and HOBr (100 μM) in water/DMSO mixtures with different water fraction (λ_{ex} =420 nm).

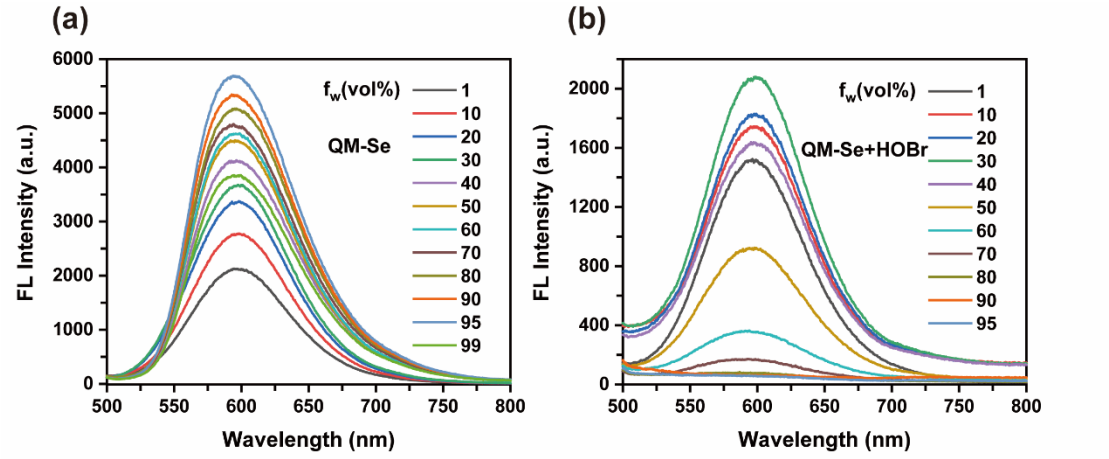

Fig. S32 (a) Fluorescent intensity of QM-Se (10 μM) in water/DMSO mixtures with different water fraction (λ_{ex} =420 nm). (b) Fluorescent intensity of QM-Se (10 μM) and HOBr (100 μM) in water/DMSO mixtures with different water fraction (λ_{ex} =420 nm).

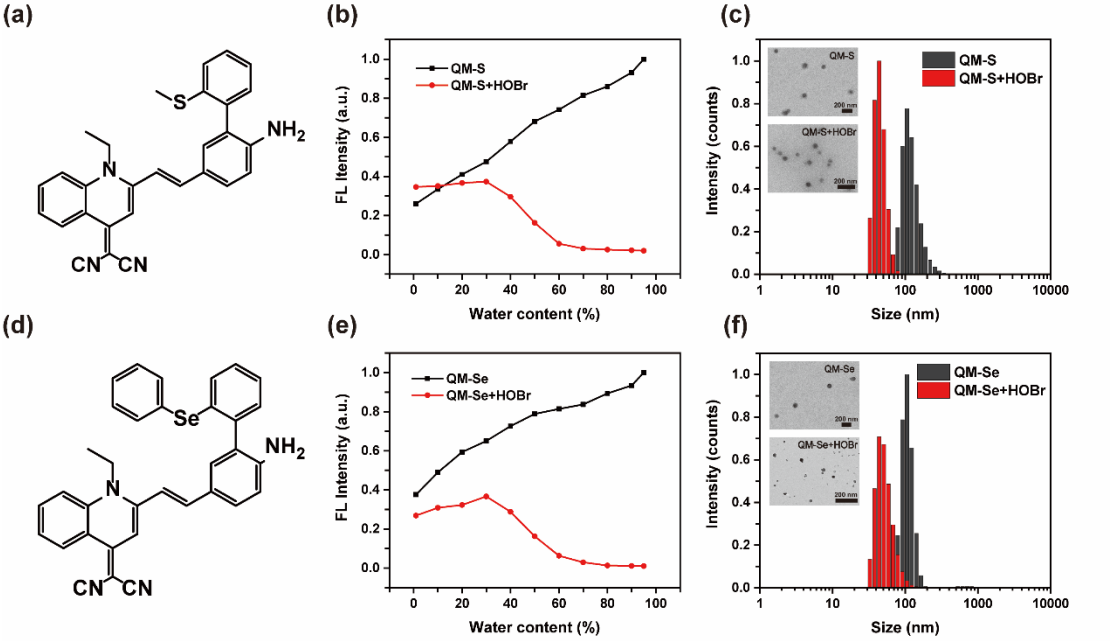

Fig. S33 The response of QM-S/QM-Se towards HOBr. (a, d) The molecular structure of QM-S/QM-Se; (b, e) the fluorescence evolution of QM-S (10 μM) and QM-Se (10 μM) aqueous solutions (water/DMSO) with different water content in the absence (black) and presence (red) of HOBr (100 μM); (c, f) DLS and TEM (inset) results of QM-S and QM-Se of the aqueous solution (water/DMSO = 95%/5%) in the absence (black) and presence (red) of HOBr.

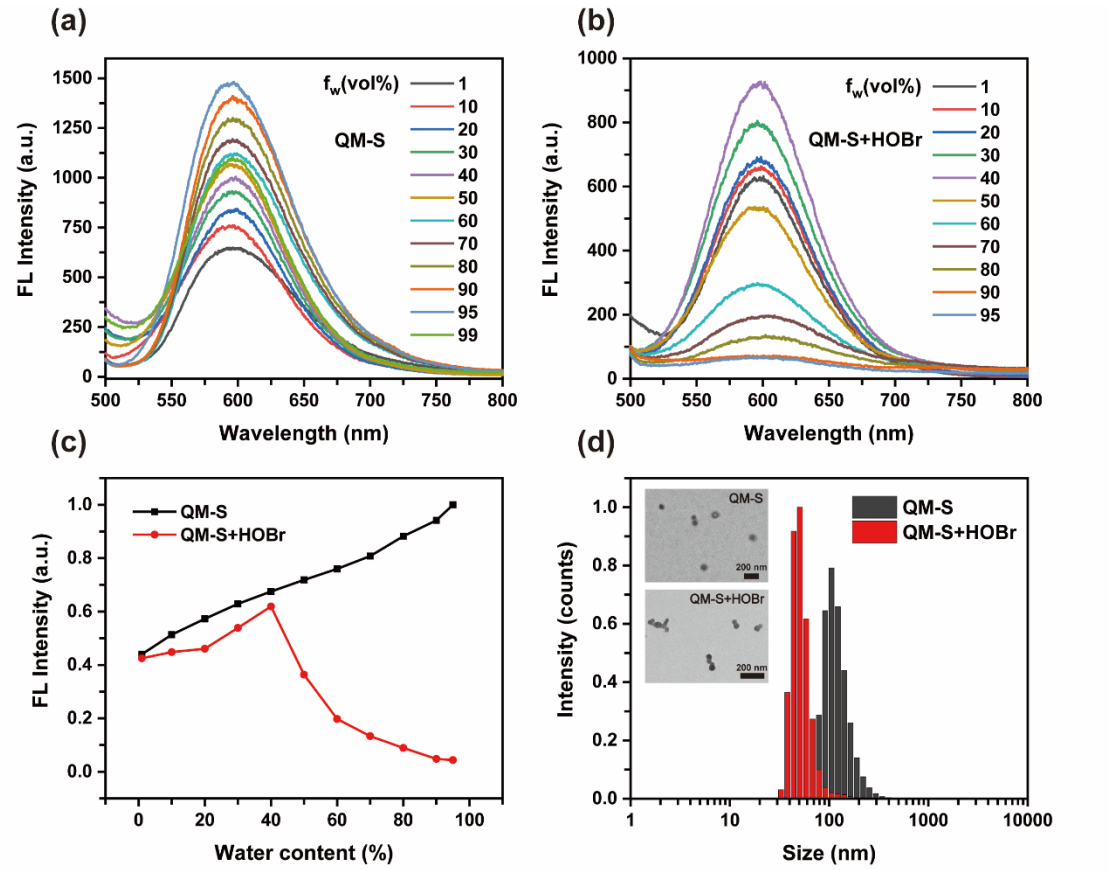

Fig. S34 (a) Fluorescent intensity of QM-S (5 μM) in water/DMSO mixtures with different water fraction (λ_{ex} =420 nm). (b) Fluorescent intensity of QM-S (5 μM) and HOBr (50 μM) in water/DMSO mixtures with different water fraction (λ_{ex} =420 nm). (c) Plot of fluorescence intensity of QM-S and QM-S+HOBr (measured at 600 nm) in water/DMSO mixtures with different water fraction. (d) DLS photographs of QM-S NPs of the aqueous solution (water/DMSO = 95%/5%) in the absence (black) and presence (red) of HOBr.

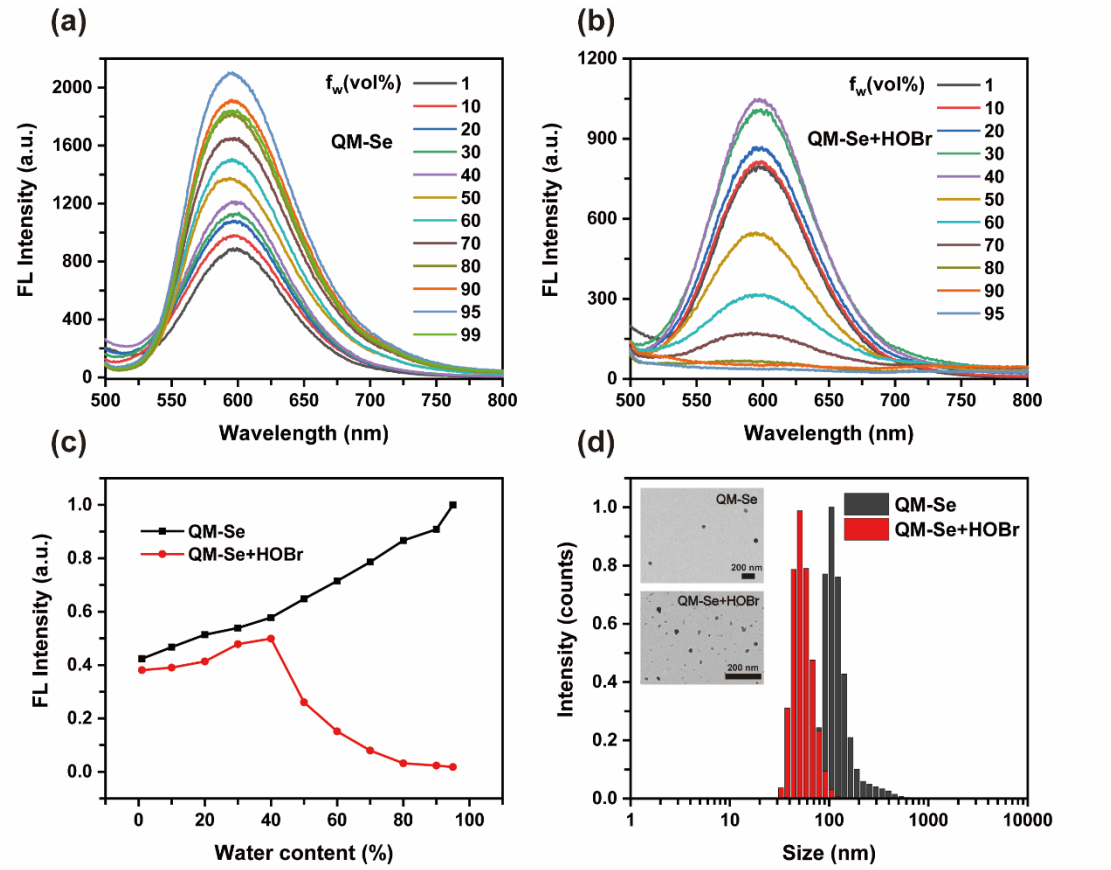

Fig. S35 (a) Fluorescent intensity of QM-Se (5 μM) in water/DMSO mixtures with different water fraction (λ_{ex} =420 nm). (b) Fluorescent intensity of QM-Se (5 μM) and HOBr (50 μM) in water/DMSO mixtures with different water fraction (λ_{ex} =420 nm). (c) Plot of fluorescence intensity of QM-Se and QM-Se+HOBr (measured at 600 nm) in water/DMSO mixtures with different water fraction. (d) DLS photographs of QM-Se NPs of the aqueous solution (water/DMSO = 95%/5%) in the absence (black) and presence (red) of HOBr.

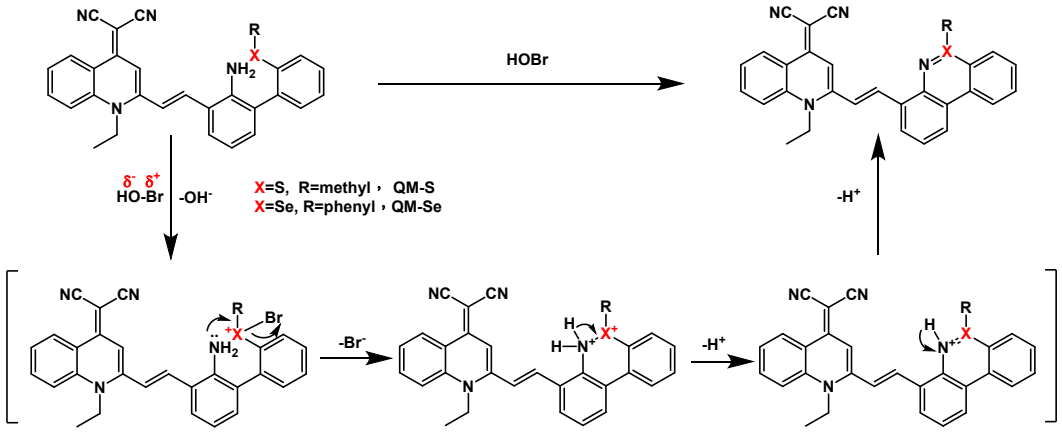

Scheme S1 The molecular structure of QM-S/QM-Se and the diagram of proposed mechanism based on the formation of S=N/ Se=N mediated by HOBr.

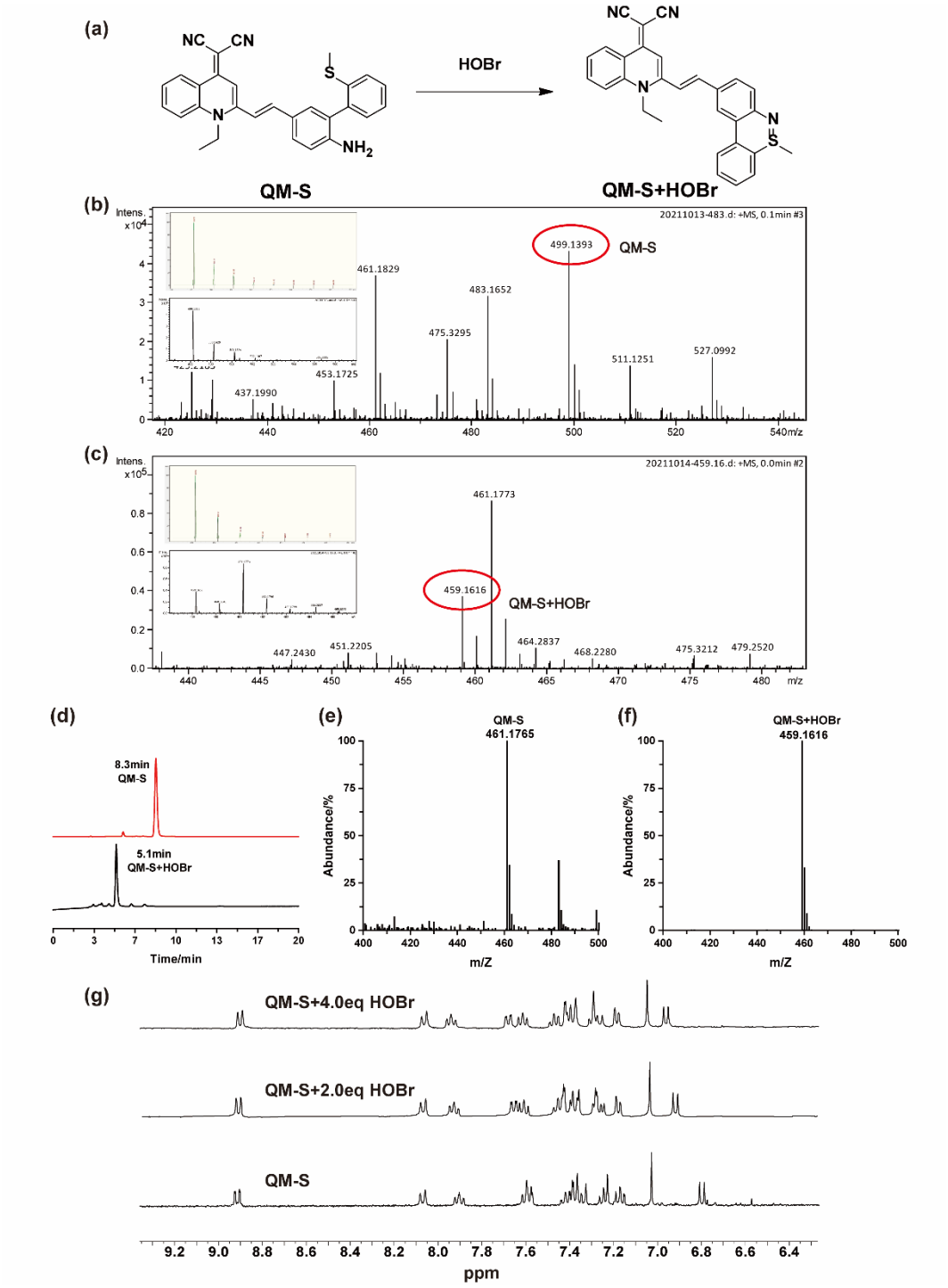

Fig. S36 Validation of the proposed mechanism for QM-S. (a, b, c) The HRMS spectra of the solution containing QM-S (10.0 μM) and HOBr (50.0 μM); insets: magnification of MS software simulation data (top) and actual MS data (bottom). (d, e, f) The HPLC-MS analysis of QM-S (60.0 μM) with/without the treatment of HOBr (300.0 μM). The mobile phase was methanol and the flow rate was 0.5 mL/min. (g) ^{1}H NMR titration (400 MHz) of QM-S with HOBr.

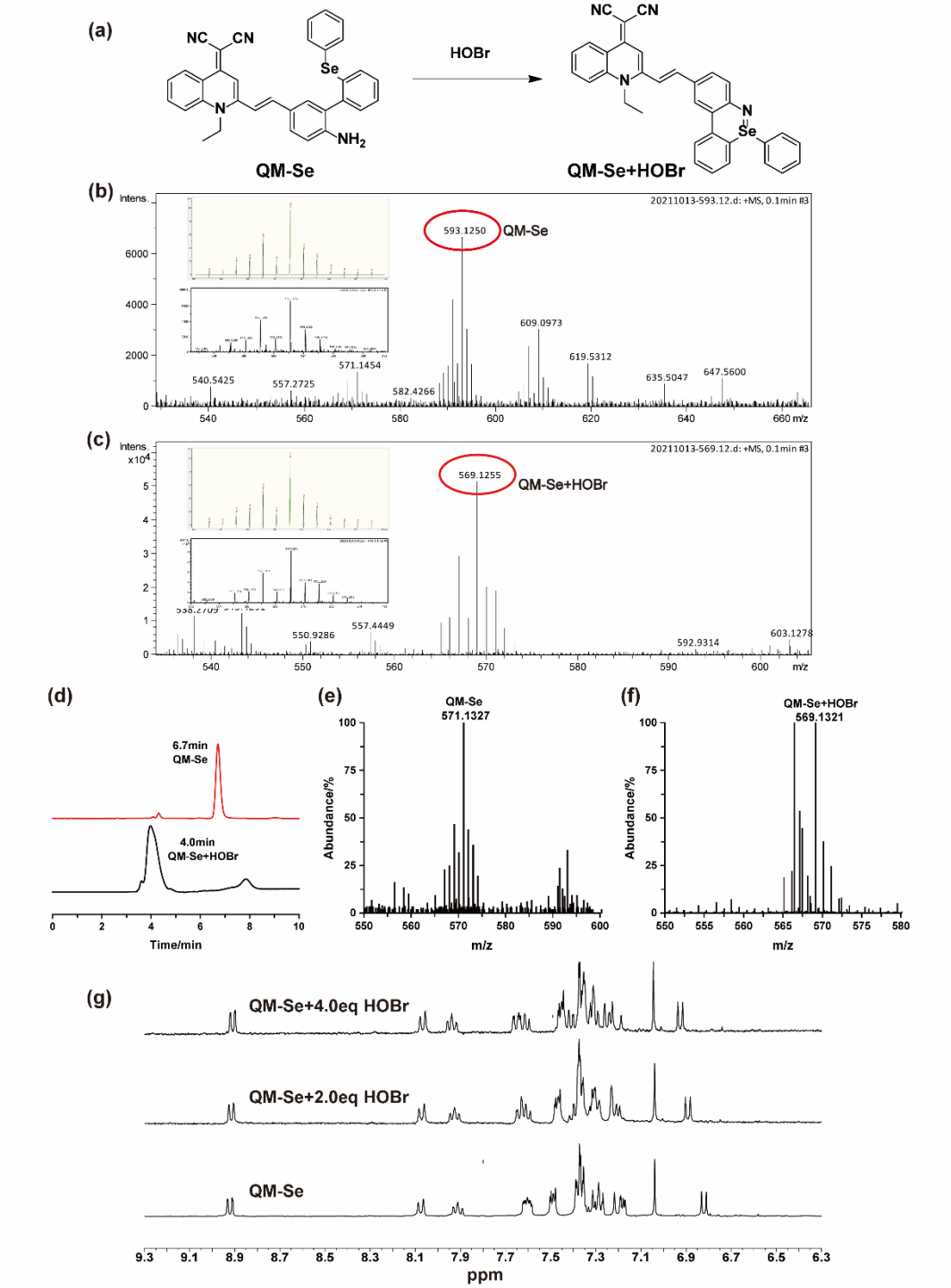

Fig. S37 Validation of the proposed mechanism for QM-Se. (a, b, c) The HRMS spectra of the solution containing QM-Se (10.0 μM) and HOBr (50.0 μM); insets: magnification of MS software simulation data (top) and actual MS data (bottom). (d, e, f) The HPLC-MS analysis of QM-Se (60.0 μM) with/without the treatment of HOBr (300.0 μM). The mobile phase was methanol and the flow rate was 0.7 mL/min. (g) ^{1}H NMR titration (400 MHz) of QM-Se with HOBr.

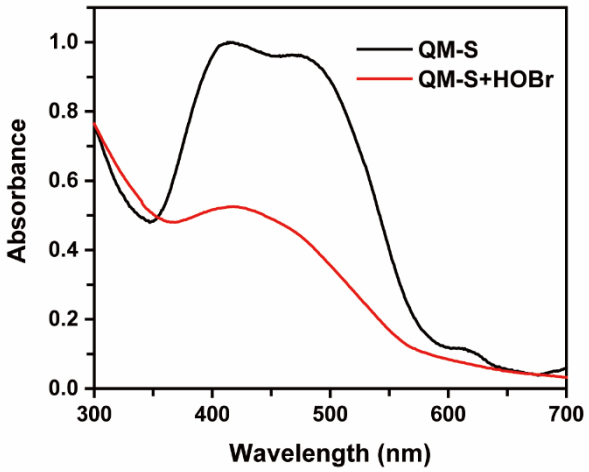

Fig. S38 Absorption spectra of QM-S (10.0 μM) in PBS buffer (1% DMSO 100 mM, pH = 7.4) before (black) and after (red) the addition of HOBr (50.0 μM).

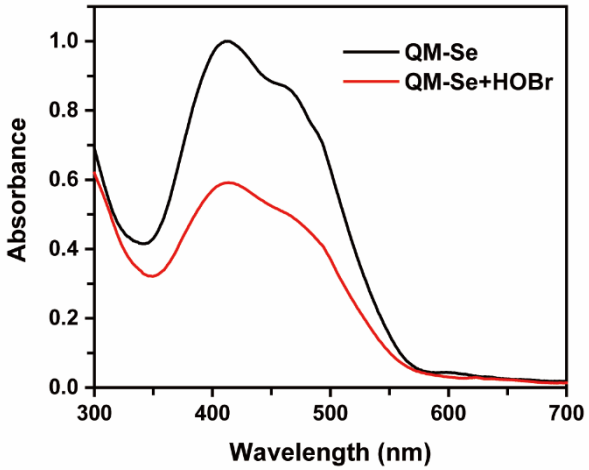

Fig. S39 Absorption spectra of QM-Se (10.0 μM) in PBS buffer (1 % DMSO 100 mM, pH = 7.4) before (black) and after (red) the addition of HOBr (50.0 μM).

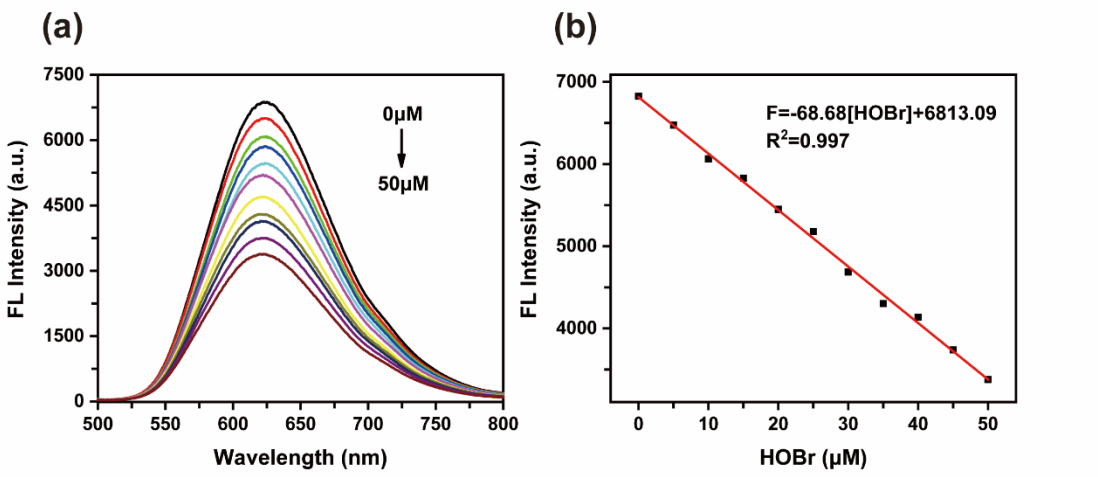

Fig. S40 Fluorescent titration assay of QM-Se (10.0 μM, $\lambda_{ex}/\lambda_{em}$=420 nm/620 nm) with HOBr (0-50.0 μM); (b) calibrated curve derived from (a).

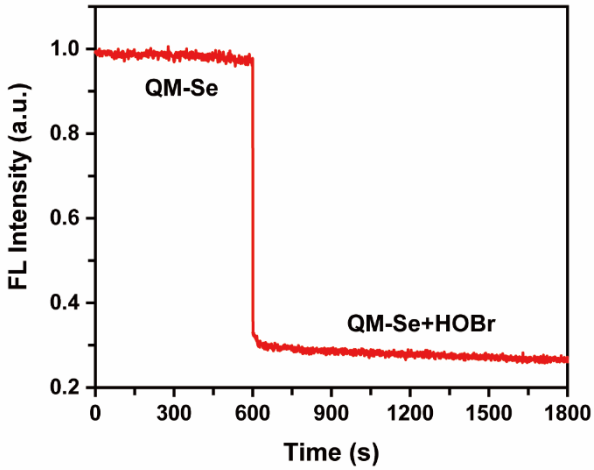

Fig. S41 Kinetic curve of QM-Se (10.0 μM) by treating with HOBr (50.0 μM). $\lambda_{ex}/\lambda_{em}$ =420 nm/620 nm.;

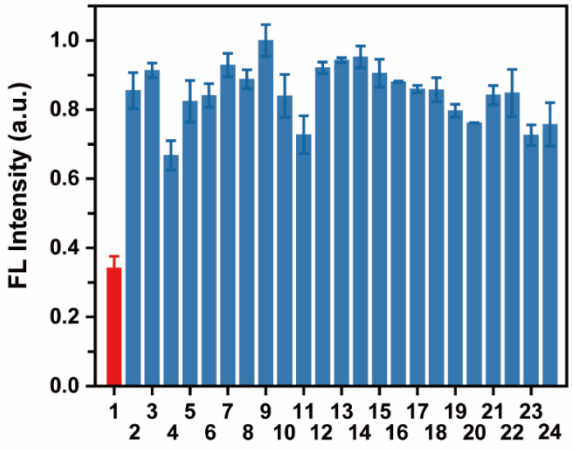

Fig. S42 Fluorescence of QM-Se (10.0 μM) in the presence of various reactive species: 1. HOBr (100.0 μM), 2. QM-S (10.0 μM), 3. H_2O_2 (200.0 μM), 4. $^1O_2$ (200.0 μM), 5. $O_2^{\bullet-}$ (200.0 μM), 6. HOCl (200.0 μM) 7. NO (200.0 μM), 8. Na_2S (200.0 μM), 9. $NaHSO_3$ (200.0 μM), 10. •OH (200.0 μM), 11. $ONOO^-$ (200.0 μM), 12. Vc (1.0 mM), 13. Cys (1.0 mM), 14. Hcy (1.0 mM), 15. GSH (1.0 mM), 16. K^+ (1.0 mM), 17. Na^+ (1.0 mM), 18. Mg^{2+} (1.0 mM), 19. Ca^{2+} (1.0 mM), 20. Cu^{2+} (1.0 mM), 21. Al^{3+} (200.0 μM), 22. Fe^{2+} (200.0 μM), 23. Fe^{3+} (200.0 μM), 24. Co^{2+} (200.0 μM). $\lambda_{ex}/\lambda_{em}$=420/620 nm。

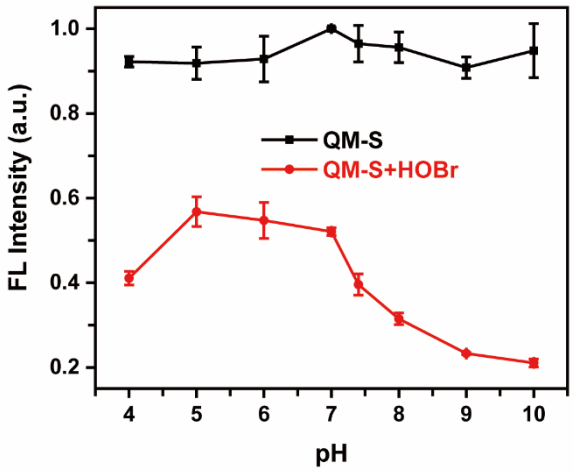

Fig. S43 Effects of pH on the fluorescence intensity of QM-S (10.0 μM) in the absence (black) and presence (red) of HOBr (100.0 μM) at room temperature. $\lambda_{ex}/\lambda_{em}$ =420 nm/600 nm.

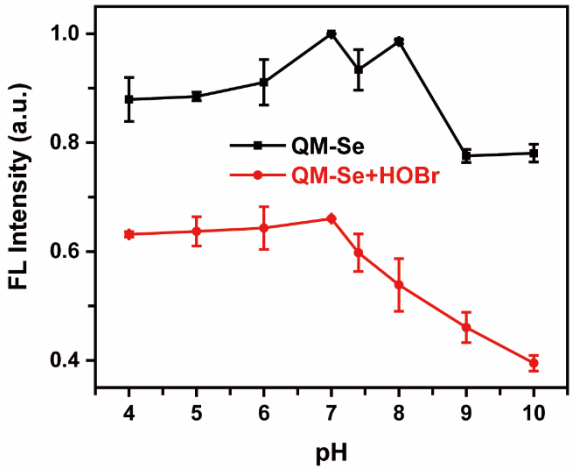

Fig. S44 Effects of pH on the fluorescence intensity of QM-Se (10.0 μM) in the absence (black) and presence (red) of HOBr (50.0 μM) at room temperature. $\lambda_{ex}/\lambda_{em}$ =420 nm/620 nm.

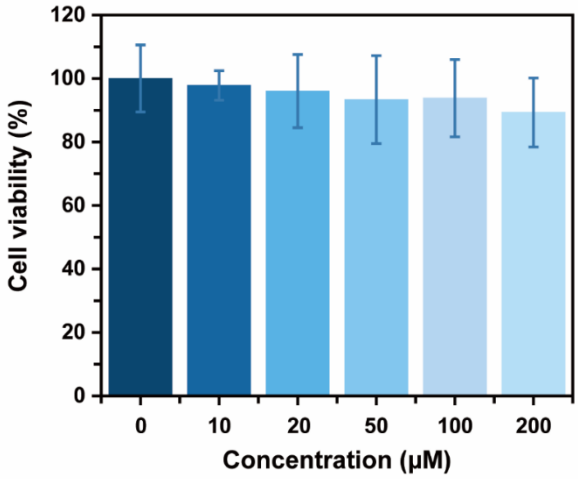

Fig. S45 MTT assay of H9C2 cells with different concentrations of QM-S (0 μM, 10.0 μM, 20.0 μM, 50.0 μM, 100.0 μM, 200.0 μM).

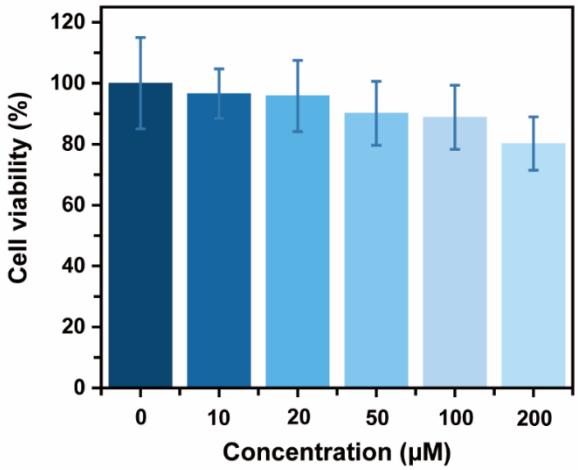

Fig. S46 MTT assay of H9C2 cells with different concentrations of QM-Se (0 μM, 10.0 μM, 20.0 μM, 50.0 μM, 100.0 μM, 200.0 μM).

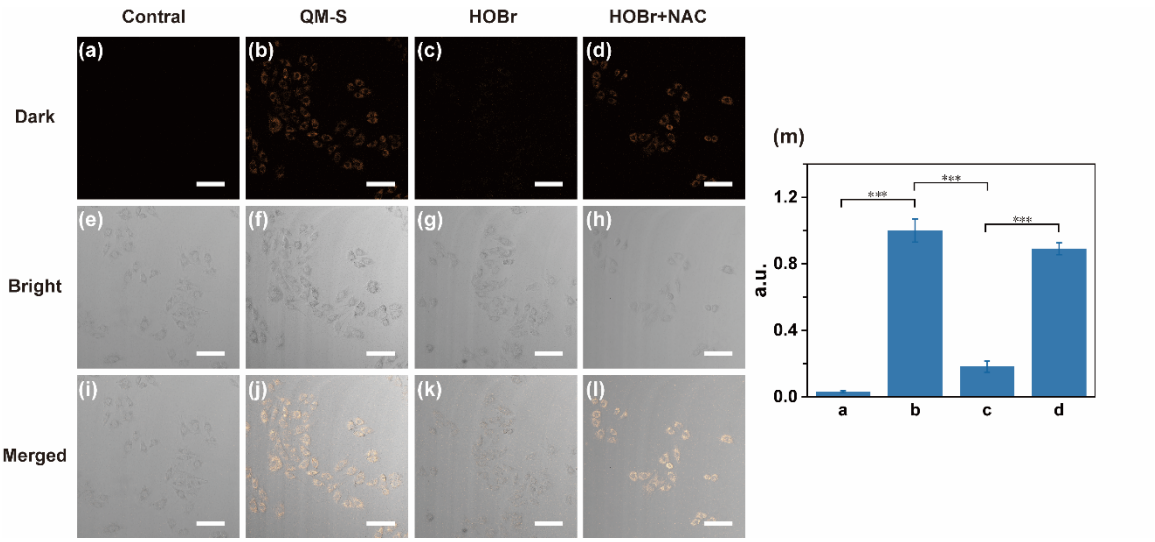

Fig. S47 CLSM images of exogenous HOBr (50.0 μM) with QM-S (5.0 μM) in H9C2 cells. $\lambda_{ex}/\lambda_{em}$=405 nm/550-645 nm. The values are the mean ± s.d. for n =3, *p < 0.05, **p < 0.01, ***p < 0.001. Scale bar: 100.0 μm.

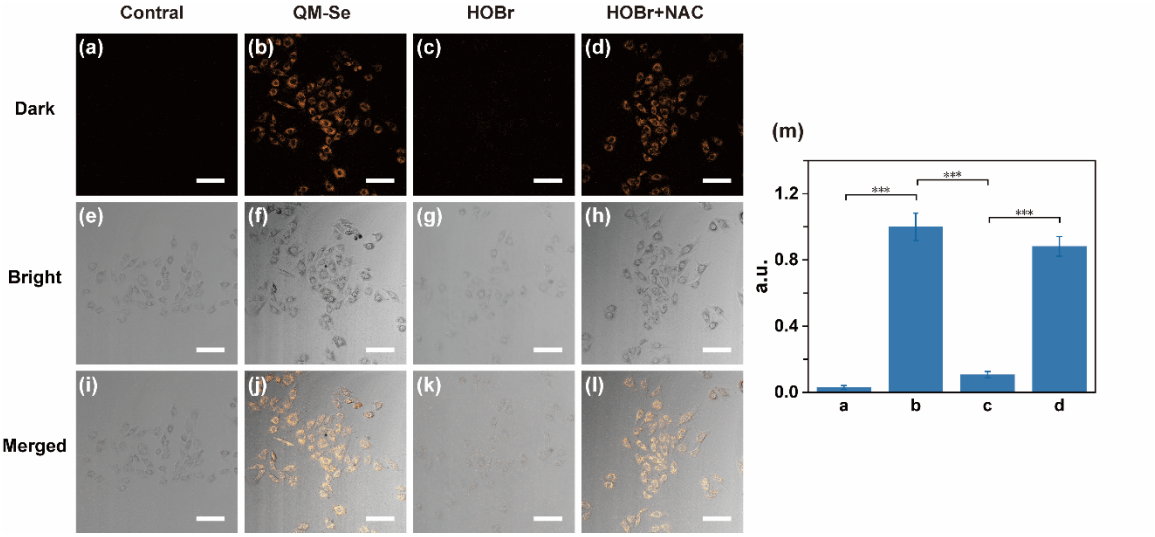

Fig. S48 CLSM images of exogenous HOBr (50.0 μM) with QM-Se (5.0 μM) in H9C2 cells. $\lambda_{ex}/\lambda_{em}$=405 nm/550-650 nm. The values are the mean ± s.d. for n =3, *p < 0.05, **p < 0.01, ***p < 0.001. Scale bar: 100.0 μm.

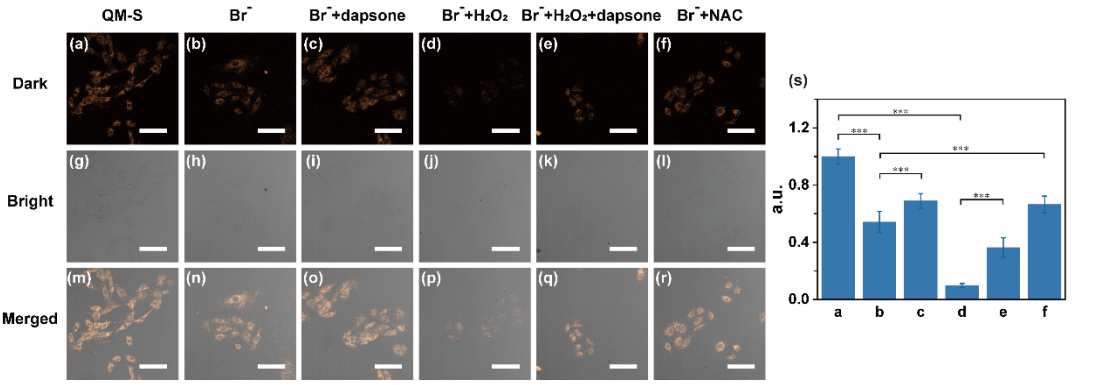

Fig. S49 CLSM of endogenous HOBr in H9C2 cells. (a, g, m) QM-S group; (b, h, n) Br^- group; (c, g, k) Br^- + dapsone group; (d, j, p) Br^- + H_2O_2 group; (e, k, q) Br^- + H_2O_2 + dapsone group; (f, l, r) Br^- + NAC group; (s) The relative fluorescence intensity of (a-f). λ_{ex} =405 nm, the collected range was 550-645 nm. The values are the mean ± s.d. for n =3, *p < 0.05, **p < 0.01, ***p < 0.001. Scale bar: 100 μm.

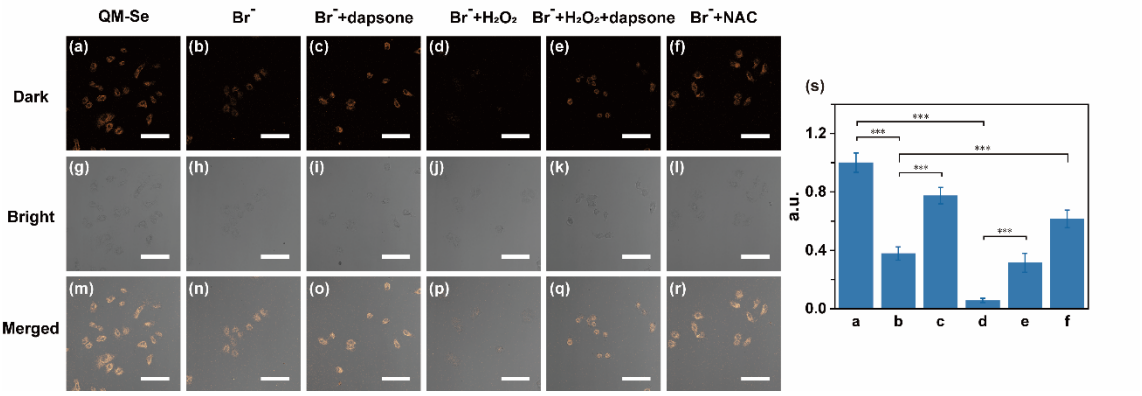

Fig. S50 CLSM of endogenous HOBr in H9C2 cells. (a, g, m) QM-Se group; (b, h, n) Br^- group; (c, g, k) Br^- + dapsone group; (d, j, p) Br^- + H_2O_2 group; (e, k, q) Br^- + H_2O_2 + dapsone group; (f, l, r) Br^- + NAC group; (s) The relative fluorescence intensity of (a-f). λ_{ex} =405 nm, the collected range was 550-650 nm. The values are the mean ± s.d. for n =3, *p < 0.05, **p < 0.01, ***p < 0.001. Scale bar: 100 μm.

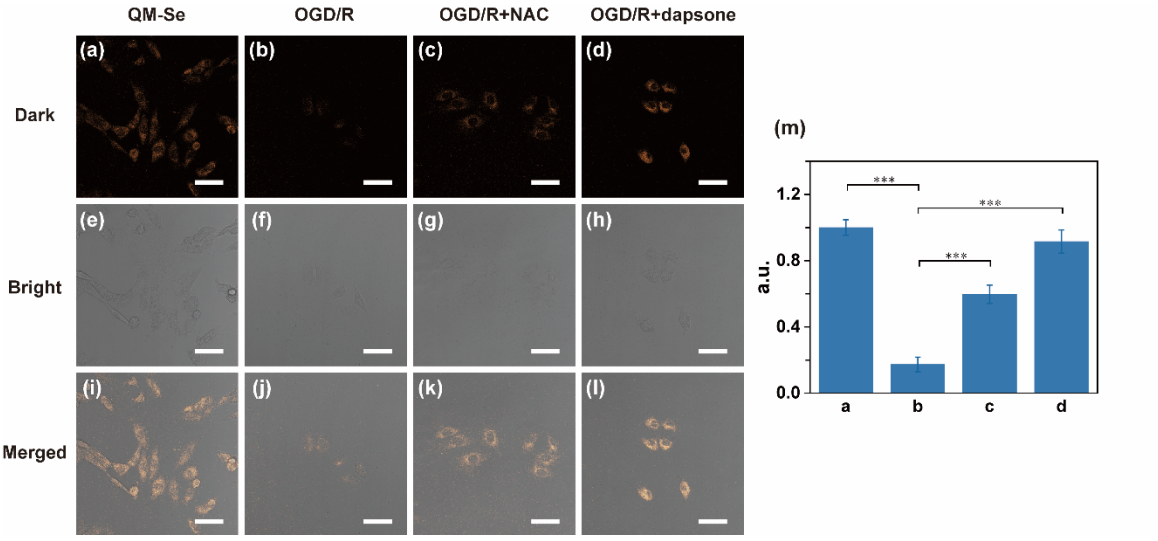

Fig. S51 CLSM of endogenous HOBr in H9C2 cells during OGD/R. (a, e, i) QM-Se group; (b, f, j) OGD/R group; (c, g, k) OGD/R + NAC group; (d, h, l) OGD/R + dapsone group; (m) The relative fluorescence intensity of (a-d). λ_{ex} =405 nm, the collected range was 550-650 nm. the values are the mean ± s.d. for n =3, *p < 0.05, **p < 0.01, ***p < 0.001. Scale bar: 50 μm.

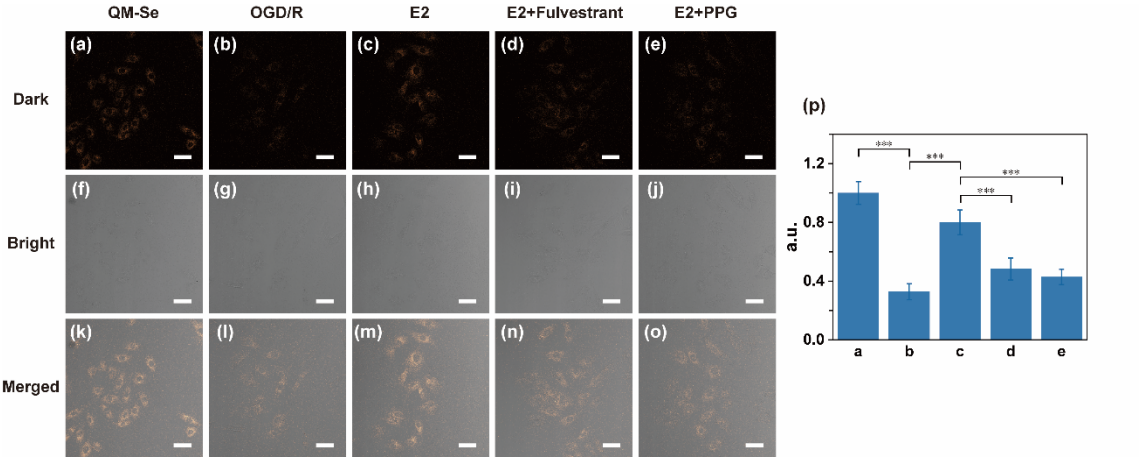

Fig. S52 CLSM of intracellular HOBr fluctuation in H9C2 cells during OGD/R and after regulating the generation of H_2S. (a, f, k) QM-Se group; (b, g, l) OGD/R group; (c, h, m) OGD/R + E2 group; (d, i, n) OGD/R + fulvestrant group; (e, j, o) OGD/R + PPG group; (p) the relative fluorescence intensity of (a-e). λ_{ex} =405 nm, the collected range was 550-650 nm. The values are the mean ± s.d. for n =3, *p < 0.05, **p < 0.01, ***p < 0.001. Scale bar: 50 μm.

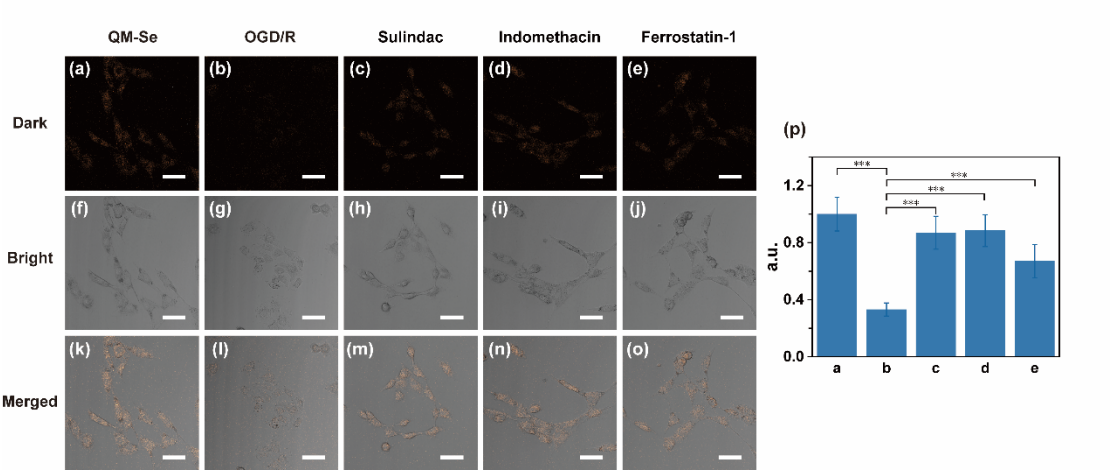

Fig. S53 CLSM of intracellular HOBr fluctuation in H9C2 cells during OGD/R and after administration of various drugs. (a, f, k) QM-Se group; (b, g, l) OGD/R group; (c, h, m) OGD/R + sulindac group; (d, i, n) OGD/R + indometacin group; (e, j, o) OGD/R + Fer-1 group; (p) the relative fluorescence intensity of (a-e). λ_{ex} =405 nm, the collected range was 550-650 nm. The values are the mean ± s.d. for n =3, *p < 0.05, **p < 0.01, ***p < 0.001. Scale bar: 50 μm.

8. References

1. Sheldrake H M, Travica S, Johansson I, et al. Re-engineering of the duocarmycin structural architecture enables bioprecursor development targeting CYP1A1 and CYP2W1 for biological activity[J]. Journal of Medicinal Chemistry, 2013, 56(15): 6273-6277.

2 Xu K, Luan D, Wang X, et al. An Ultrasensitive cyclization-based fluorescent probe for imaging native HOBr in live cells and zebrafish[J]. Angewandte Chemie International Edition, 2016, 55(41): 12751-12754.

3. Han X, Yang X, Zhang Y, et al. A novel activatable AIEgen fluorescent probe for peroxynitrite detection and its application in EC1 cells[J]. Sensors and Actuators B: Chemical, 2020, 321: 128510.

4. Chang M, Yan C, Shi L, et al. Rational design of shortwave infrared (SWIR) fluorescence probe: Cooperation of ICT and ESIPT processes for sensing endogenous cysteine[J]. Chinese Chemical Letters, 2022, 33(2): 762-766.

5. Tuccitto N, Catania G, Pappalardo A, et al. Agile detection of chemical warfare agents by machine vision: A supramolecular approach[J]. Chemistry-A European Journal, 2021, 27(55): 13715-13718.